Molecular Catalysis 541 (2023) 113113

Contents lists available at ScienceDirect

Molecular Catalysis

journal homepage: www.journals.elsevier.com/molecular-catalysis

Metallic and non-metallic components and morphology of iron-based catalytic effects for selective catalytic reduction performance: A systematic review

Longteng Yuan [a,c], Ping Hu [a,b,c,*], Boliang Hu [a,b,*], Jiayu Han [a,b], Shengjie Ma [a,c], Fan Yang [a,b], Alex A. Volinsky [d]

[a] National and Local Joint Engineering Research Functional Center for Materials Processing, Xi'an University of Architecture and Technology, Xi'an 710055, China
[b] School of Metallurgy Engineering, Xi'an University of Architecture and Technology, Xi'an 710055, China
[c] School of Mechanical and Electrical Engineering, Xi'an University of Architecture and Technology, Xi'an 710055, China
[d] Department of Mechanical Engineering, University of South Florida, 4202 E. Fowler Ave., ENG 030, Tampa, FL 33620, USA

ARTICLE INFO

Keywords:
NH_3-SCR
Fe-based catalyst
NO_x removal
Metallic component
Non-metallic component
Morphological structure

ABSTRACT

Selective catalytic reduction (SCR) has been widely used to remove NO_x from automobile exhaust and industrial production. Fe-based catalysts with low cost, high activity, and excellent SCR performance have become an active research topic in recent years. The latest research progress of NO_x removal by the NH_3-SCR method using Fe-based catalysts is summarized. The effects of synergistic interaction between Fe and other elements are analyzed in terms of the redox performance, surface acidity, and catalytic activity of catalysts. In addition, the effects of catalyst morphology and structure on SCR performance are analyzed. Finally, according to the research results of Fe-based catalysts in the laboratory, some practical application problems are considered.

1. Introduction

Living standards have been improving with the continuous development of science and technology. However, the corresponding environmental pollution is becoming more serious. Specifically, the flue gas emitted from industrial production and automobile exhausts has been causing serious atmospheric pollution. Industrial and automotive emissions include carbon monoxide (CO), nitrogen oxides (NO_x), hydrocarbons (C_xH_y), sulfur oxides (mainly SO_2), and particulate matter (PM) [1,2]. As one of the main sources of air pollution, NO_x can irritate the lungs, making it harder to fight respiratory diseases such as common colds. At the same time, NO_x, mainly nitric oxide (NO) and nitrogen dioxide (NO_2), are important substances that form photochemical smog and acid rain [3,4]. Therefore, reducing NO_x emissions is of great significance to the environment.

In recent years, methods commonly used to remove NO_x include a selective catalytic reduction (SCR), and NO_x storage and reduction (NSR). The main reducing agents used to remove NO_x by the SCR method are H_2, C_xH_y, and urea (NH_3) [5–7]. NH_3 selective catalytic reduction (NH_3-SCR) technology is the most promising for the purification of NO_x from diesel engines and industrial pollution emissions [8]. The main method is to pass NH_3 or urea aqueous solution as a reducing agent into the pipeline to react with the polluted NO_x gas to generate non-polluting N_2 and H_2O, thereby reducing toxic emissions. Since the 1970s, NH_3-selective catalytic reduction of NO_x (NH_3-SCR) has been widely used in NO_x emission control due to its high efficiency and excellent selectivity [9–11]. The currently commercialized NH_3-SCR catalyst is V_2O_5-WO_3(MoO_3)/TiO_2, which has high NO_x activity at 300–400 °C [8,12]. However, these catalysts are prone to form nitrous oxide (N_2O) and produce vanadium poisoning at high temperatures and have the disadvantages of poor low-temperature activity, high operating temperature, and narrow operating temperature window [13–18]. Therefore, the current research direction is mainly to develop low-temperature high-activity, low-cost, and environmentally-friendly SCR catalysts [11,19,20].

Due to the unsaturation of the Fe *d* electron orbital and the coupling effect of Fe^{3+} and Fe^{2+}, it is easy to transfer electrons and promote the NH_3-SCR reaction at low temperatures. Thus, Fe has excellent redox ability. In addition, owing to abundant reserves, low cost, non-toxicity, and environmental friendliness, Fe is widely used in SCR catalysts

* Corresponding authors at: National and Local Joint Engineering Research Functional Center for Materials Processing, Xi'an University of Architecture and Technology, Xi'an 710055, China.
E-mail addresses: huping1985@126.com (P. Hu), huboliang@xauat.edu.cn (B. Hu).

https://doi.org/10.1016/j.mcat.2023.113113
Received 20 January 2023; Received in revised form 6 March 2023; Accepted 23 March 2023
Available online 28 March 2023

[21–25]. In general, Fe-based metal oxide catalysts have lower costs and stronger thermal stability than noble metal catalysts. Therefore, in the research of NH_3-SCR catalysts in the laboratory, a lot of research on Fe-based catalysts has been carried out. However, it is still challenging to work with Fe-based catalysts under real conditions because of their insufficient low-temperature activity, NH_3 oxidation at high temperatures, and many side reactions. Thus, they need to be modified to improve low-temperature catalytic activity, surface acidity, and selectivity [26–28].

This paper reviews the research progress of Fe-based catalysts for NO_x removal by NH_3-SCR in recent years and summarizes the modification of Fe-based catalysts by metal and non-metal elements, including the adjustment of the redox characteristics, surface acidity, and catalytic performance of Fe-based catalysts through inter-element synergy, as well as the effects of morphological structure on the NH_3-SCR activity of Fe-based catalysts (Fig. 1). Finally, the existing problems and future development directions of Fe-based catalysts are systematically reviewed.

2. Reaction mechanism of Fe-based transition metal oxide catalysts

At present, the reaction mechanism of the catalyst is mainly carried out by in-situ diffuse reflectance infrared spectroscopy (DRIFT). The structural change of the sample is characterized under the condition of being in situ, and then the dynamic change of the adsorbed species on the surface of the catalyst during the catalytic reaction is studied, and the intermediate signal during the catalytic process is observed. The reaction mechanism of Fe-based catalysts was studied by in situ DRIFT to more intuitively explore the adsorption, activation and reaction of the catalyst surface during the reaction process. In addition, scholars generally believe that the SCR reaction on transition metal oxide catalysts has two mechanisms, namely the Langmuir-Hinshelwood (L-H) and the Eley-Rideal (E-R) mechanisms [33,34]. Based on these mechanisms, extensive research has been conducted to analyze their advantages and disadvantages. Generally speaking, NO_x is removed by the NH_3-SCR method, and two NO_x and NH_3 gasses are mainly involved in the reactions. As shown in Fig. 2(a), in a typical L-H mechanism, the active sites on the catalyst surface can simultaneously adsorb NH_x and NO_x species, and then the two adsorption states can directly react to generate NH_4NO_x, which is then decomposed into N_2 and H_2O on the catalyst surface. As shown in Fig. 2(b), in the E-R mechanism, the catalyst only adsorbs NH_3 species, that is, the active sites on the catalyst surface only adsorb NH_x species, and the adsorbed NH_x species can directly react with gaseous NO_x species to generate NH_4NO_x, which is subsequently decomposed into N_2 and H_2O. The activation energy required for the adsorbed species to participate in the SCR reaction is low, and the reduction reaction is easy to occur at low temperatures. The active sites of the catalyst continuously complete the redox cycle in SCR reaction. In addition, two reaction mechanisms often coexist in SCR reaction on the catalyst, and in-depth study of the reaction mechanism can better optimize the catalyst modification.

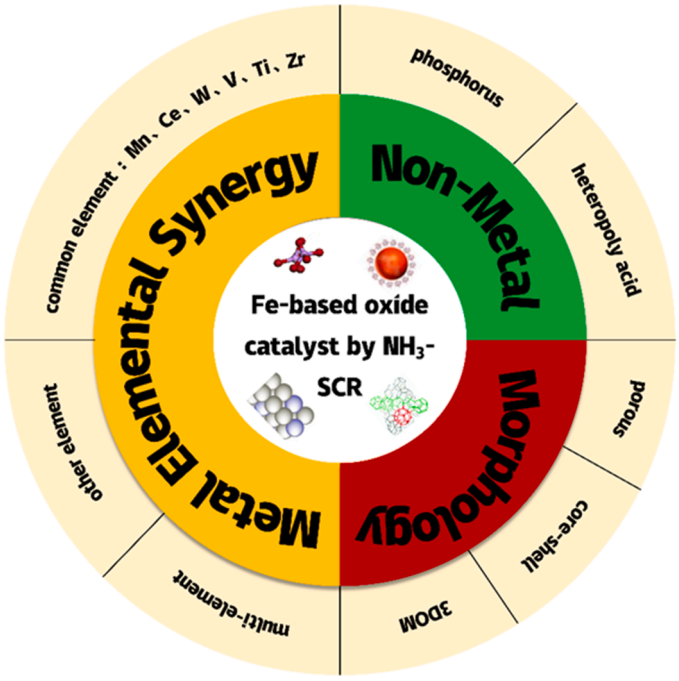

Fig. 1. Modification methods of iron-based catalysts [29–32].

At 200 ℃, $Fe_{0.2}Mn_{0.8}TiO_x$ catalyst mainly follows the L-H mechanism. Lewis acid and Brønsted acid on the catalyst surface can adsorb NO_x and NH_3, and the adsorption state of monondonts nitrate species and NH_4^+ on the B acid site are always in reaction [35]. The NH_3-SCR reaction of $Cu_{0.02}Fe_{0.2}W_{0.02}TiO_x$ catalyst at 130 ℃ or 240 ℃ mainly follows the Eley-Rideal mechanism, and the adsorbed nitrate species are stable and not easy to participate in the reaction [36]. Whether the type of catalyst is the key factor leading to the difference in the reaction mechanism of the catalyst. γ-Fe_2O_3 catalyst is an E-R reaction mechanism, and SCR reaction mainly occurs between Lewis acid site and gaseous NO_x. After Mo is added, L-H mechanism and E-R mechanism coexist [37]. The reaction mechanism of Mn(0.4)/TiO_2 catalyst studied by Wu et al. is E-R reaction mechanism. However, when Fe was added to the catalyst, the bidentate nitrate adsorbed on the surface of Fe(0.1)-Mn (0.4)/TiO_2 catalyst was converted to monocentate nitrate, which could react with NH_4^+ ions [38]. The results showed that the reaction mechanism of the catalyst changed to the coexistence of L-H mechanism and E-R mechanism. In addition, the same mechanism can also affect the catalytic activity of catalysts. Both MnO_x-FeO_x nanoparticles and MnO_x-FeO_x nanoneedles follow the E-R mechanism and L-H mechanism simultaneously. However, their catalytic effects are completely different. Because of the strong adsorption capacity of Lewis and Brønsted acid sites on the surface of nanoneedles, the adsorbed species can participate in the reaction more easily [39].

Since the pollutants emitted by automobiles and factories are often accompanied by toxic substances such as SO_2, alkali and heavy metals, when the catalyst adsorbs the reaction gas, the toxic substances will compete with the reaction gas for adsorption, resulting in decreased SCR activity of the catalyst. Some studies say that NO_x and SO_2 will produce competitive adsorption at the active site [40]. When the catalyst is E-R reaction mechanism, the side effects of competitive adsorption are significantly reduced [30]. Therefore, the reduction of competitive adsorption of toxic substances and reactive species is an effective method to improve the activity of SCR catalysts. Changing the reaction mechanism of the catalyst by element modification can often effectively suppress the deactivation of the catalyst's active sites, thereby increasing the service life of the catalyst. Therefore, further analysis of the effects of element modification on the reaction mechanism of Fe-based catalysts has far-reaching significance.

3. Effects of element modification on Fe-based oxide catalysts

3.1. Synergy between metal oxides and Fe-based oxide catalyst

Fe-based catalysts have excellent high-temperature activity and hydrothermal stability and are more promising for practical applications than other metal oxide catalysts. However, pure Fe_2O_3 catalyst has low activity and a narrow temperature window, with the highest NO conversion efficiency of only 48% at 330 °C Fig. 3) [41]. After the NO conversion rate of Fe_2O_3 reaches the maximum value at 330 °C, it shows a downward trend with further temperature increase. The key lies in the low-temperature redox performance and insufficient acid sites of single

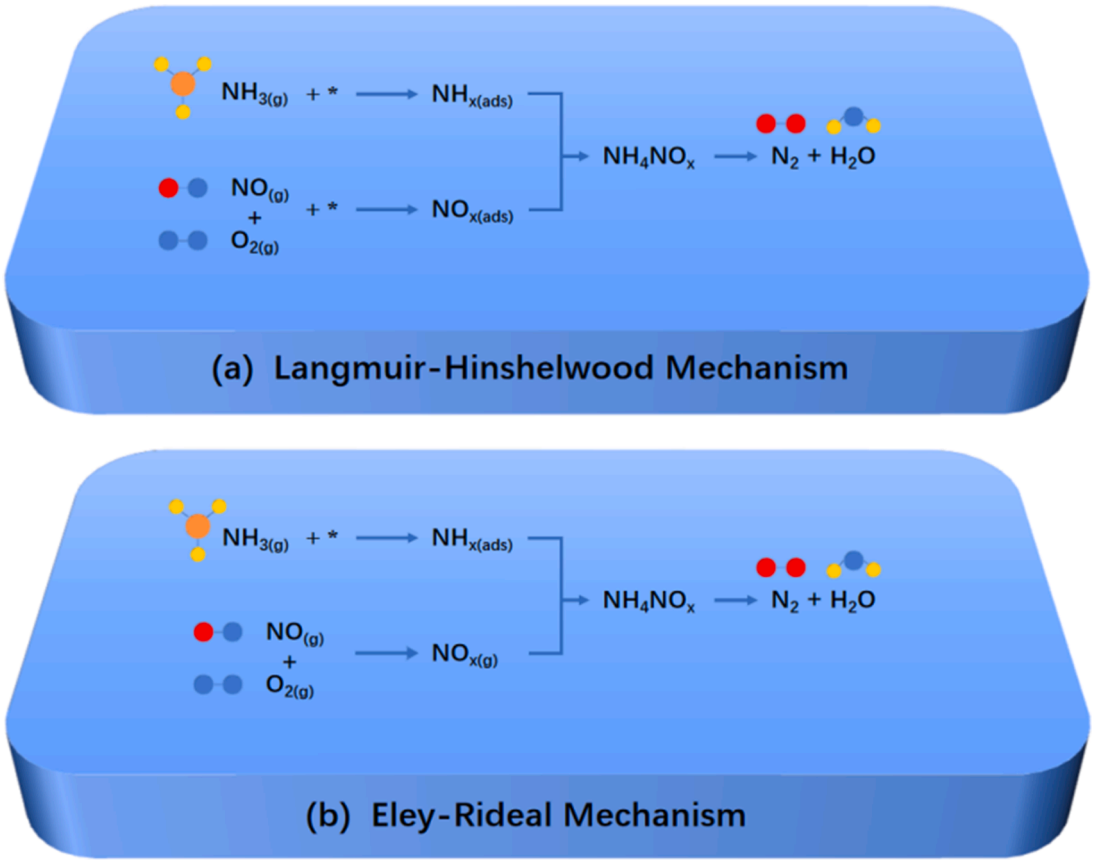

Fig. 2. (a) Langmuir-Hinshelwood and (b) Eley-Rideal reaction mechanisms of catalysts.

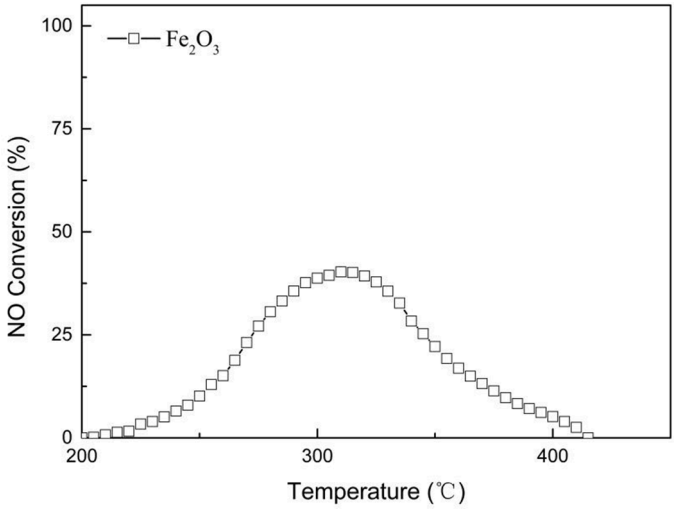

Fig. 3. NO conversion of pure Fe_2O_3 [41].

iron oxide, the narrow temperature window, and the easy non-selective oxidation of NH_3 at high temperatures (Eqs. 1–(3). Therefore, other metals are often used to modify the redox properties and surface acidity of Fe-based catalysts to obtain catalysts with better de-NO_x activity. The elements commonly used to improve the de-NO_x performance of Fe-based catalysts are Mn, W, Ce, Ti, V, Zr, and other metals.

$$4NH_3+4O_2\rightarrow 2N_2O+6H_2O \quad (1)$$

$$4NH_3+5O_2\rightarrow 4NO+6H_2O \quad (2)$$

$$4NH_3+6O_2\rightarrow 4NO_2+6H_2O \quad (3)$$

3.1.1. *Synergy between mno$_x$ and FeO$_x$*

Among transition metals, Mn has various valence states and excellent redox properties because of the easy transfer of electrons in the *d* orbitals [42–44]. In addition, the Mn-based catalyst has excellent de-NO_x performance at low temperatures, but the N_2 selectivity and SO_2 resistance at high temperatures are low, and the strong interaction with Fe can effectively improve its shortcomings and the low-temperature activity of the Fe-based catalyst. This is discussed below and summarized in Table 1 for the NH_3-SCR catalytic performance of different Fe-Mn catalysts.

The physical and chemical characteristics of Fe-Mn catalysts are different under different preparation methods, resulting in different SCR activities among Fe-Mn catalysts. The NO_x conversion rate of the Mn-Fe catalyst prepared by co-precipitation method exceeds 80% at 150–200 °C [45]. The NO_x conversion rate of three-dimensional ordered microporous (3DOM) Fe_1_Mn_3—O_x catalyst prepared by the colloidal crystal template method was over 80% at 302–485 °C [46]. The high conversion of the catalyst is attributed to the synergism between Fe and Mn, which enhances the electron transfer rate of the catalyst and promotes the redox cycle ($Fe^{3+}+Mn^{3+}\Leftrightarrow Mn^{4+}+Fe^{2+}$). So far, some low-cost natural minerals rich in iron can also be used as raw materials to prepare Fe-based catalysts. The NO_x conversion rate of 3% Mn-siderite ($FeCO_3$) catalyst is higher than 90% at 180–300 ℃ [47]. The interaction between Mn and Fe in a 3% Mn-siderite catalyst also inhibited the agglomeration of MnO_2. NO conversion of Fe-Mn catalysts prepared from natural manganese-rich limonite is higher than 90% in the temperature range of 130–300 ℃ [48]. We noticed that these natural minerals, which are widely found on the Earth's surface and have low cost, have excellent activity in NH_3-SCR reaction for NO_x removal, and can be used as catalyst raw materials in the future.

Table 1
NH_3-SCR activities of different Fe-Mn catalysts.

Catalyst	Temperature window	NO_x conversion	Reaction conditions	Refs.
Mn-Fe	150–200 °C	>80%	500 ppm NH_3, 500 ppm NO, 5% O_2, 30,000 h^{-1}, 100 ml/min	[45]
3DOM Fe_1_Mn_3—O_x	302–485 °C	>80%	1000 ppm NH_3, 1000 ppm NO, 3% O_2, 50 ml/min	[46]
3%Mn-($FeCO_3$)	180–300 °C	>90%	500 ppm NH_3, 500 ppm NO, 3% O_2, 10,000 h^{-1}, 1.5 L/min	[47]
H300 Fe-Mn	130–300 °C	>90%	1000 ppm NH_3, 1000 ppm NO, 3% O_2, 72,000 h^{-1}, 300 ml/min	[48]
20%Mn-10%Fe/TiO_2(SD)	80–150 °C	>95%	500 ppm NH_3, 500 ppm NO, 5% O_2, 24,000 $mLg^{-1}h^{-1}$, 800 ml/min	[49]
$Fe_{0.3}Mn_{0.8}/TiO_2$	200–250 °C	>97%	400 ppm NH_3, 400 ppm NO, 4% O_2, 50,000 h^{-1}	[50]
8Fe-8Mn/Al_2O_3	90–210 °C	>92.6%	500 ppm NH_3, 500 ppm NO, 3% O_2, 1500 ml/min	[51]
$Mn_1Fe_{0.25}Al_{0.75}O_x$	80–250 °C	>88%	500 ppm NH_3, 500 ppm NO, 5% O_2, 60,000 $mLg^{-1}h^{-1}$, 200 ml/min	[52]

Interestingly, Fe and Mn elements can also produce strong interactions when used as active components of catalysts and loaded on different supports. The NO conversion rate of Mn-Fe/TiO_2 (SD) catalyst prepared with TiO_2 as the support is greater than 95% at 80–150 ℃ [49]. The NO conversion rate of Fe-MnOx/TiO_2 catalyst synthesized by sol-gel method is about 97% at 200–250 ℃ [50]. The presence of Fe can increase the BET surface area and promotes the morphological transformation of MnO_x from crystalline to amorphous. It is widely used as catalyst support due to the excellent acidity of the Al_2O_3 surface. The 8Fe-8Mn/Al_2O_3 catalyst has a NO conversion rate of over 92.6% in the temperature range of 90–210 ℃. [51]. It is attributed to the interaction between Fe and Mn that promotes the formation of Fe^{3+}. A new $Mn_1Fe_{0.25}Al_{0.75}O_x$ catalyst by calcination of $Mn_1Fe_{0.25}Al_{0.75}$—NO_3 layered double hydroxide (LDH) precursor, and the NO_x conversion rate was higher than 88% at 80–250 °C [52]. The addition of Fe promoted the mobility of adsorbed oxygen on the surface.

However, it was found that the appropriate addition of the Mn could produce a good interaction with the Fe, thus promoting the SCR activity of the catalyst. However, it is not known exactly how Mn promotes Fe. Therefore, Ren et al. used density functional theory (DFT) to study the mechanism of NO_x removal by the SCR method on Mn-doped γ-Fe_2O_3 catalyst and the effects of Mn doping on the SCR process [53]. It turns out that the Fe-O bond is longer than the Mn-O bond, which means that there is an electron transfer from the Mn cation to the Fe cation. In addition, Fe is more electronegative than Mn, so the doping of Mn will bring more valence electrons and be attracted to Fe, increasing the surface free electrons and thus changing the surface redox capacity.

In general, Mn has excellent SCR activity at low temperatures, but the catalytic activity and N_2 selectivity are often insufficient at high temperatures, and the operating temperature window is narrow, while the Fe element is the opposite. Therefore, the combination of Mn and Fe leads to the interaction between Mn and Fe, which effectively improves the low-temperature SCR activity and N_2 selectivity of metal oxide catalysts, which is mainly attributed to the effective electronic synergy between Mn and Fe ions (Fe^{3+}+Mn^{3+}⇔Mn^{4+}+Fe^{2+}), improving the redox properties of the catalyst. At the same time, the transformation of MnO_x and FeO_x from crystalline to amorphous state is promoted, and their dispersion on the catalyst surface is improved. All these factors together contribute to the excellent SCR performance of the catalyst.

3.1.2. *Synergy between WO_x and FeO_x*

Tungsten oxide (WO_3) is commonly used as an activity modifier for the NH_3-SCR catalysts, owing to its inherent thermal stability, high surface activity, and excellent high-temperature SCR activity [36,54,55]. After adding tungsten to other phases, the dispersion and stability of the active phase can be improved, the surface activity can be increased, the redox performance can be adjusted, and the NH_3-SCR activity can be enhanced. Therefore, W is commonly used to modify the Fe element to enhance its dispersion and improve its acid site strength, thereby promoting the SCR activity of the catalyst. The NH_3-SCR performance of different Fe-W catalysts is listed in Table 2.

It has been reported that 10% WO_3/Fe_2O_3 [56] and 5% WO_3/Fe_2O_3 [57] catalysts prepared by the same preparation method also have different SCR activities due to the different interactions between WO_x and FeO_x in the prepared W-Fe catalysts. The NO_x conversion rate of 10% WO_3/Fe_2O_3 catalyst is more than 90% at 275–425 ℃. The NO_x conversion rate of 5% WO_3/Fe_2O_3 catalyst exceeds 80% at 300–450 ℃. Same point is that they all found that there is a strong interaction between WO_x and Fe_2O_3: (1) High dispersion of WO_x on the surface of Fe_2O_3; (2) The redox performance of the catalyst is improved; 3) It is helpful to increase the number and intensity of acidic sites. However, the difference is that the presence of WO_3 on 10% WO_3/Fe_2O_3 catalyst [56] inhibits the crystallization of the Fe_2O_3 phase and helps to improve the specific surface area of Fe_2O_3. In addition, both catalysts are E-R reaction mechanisms, but the interaction between the two elements in the 5% WO_3/Fe_2O_3 catalyst [57] mainly enhanced the strength of Lewis acid sites on the catalyst, rather than simultaneously enhancing the strength of Lewis and Brønsted acid sites. This may be the stronger adsorption and activation of NH_3 by Lewis acid sites in the E-R mechanism of the W-Fe catalyst. The 30% WO_3/Fe_2O_3 catalyst achieved a NO_x removal rate close to 100% at 225–500 °C [29]. As shown in Fig. 4, the doping of WO_3 can effectively inhibit the growth of Fe_2O_3 particles, but also leads to particle agglomeration. Although the SCR activity of the Fe-W catalyst is excellent, scholars have not pointed out the active center of the Fe-W catalyst, possibly because the particles are irregular and have different shapes, which is difficult to locate from the atomic perspective. Zhang

Table 2
NH_3-SCR activities of different Fe-W catalysts.

Catalyst	Temperature window	NO_x conversion	Reaction conditions	Refs.
10% WO_3/Fe_2O_3	275–425 °C	>90%	500 ppm NH_3, 500 ppm NO, 5% O_2, 100,000 h^{-1}, 300 cm^3/min	[56]
5% WO_3/Fe_2O_3	300–450 °C	>80%	500 ppm NH_3, 500 ppm NO, 5% O_2, 50,000 h^{-1}, 500 ml/min	[57]
30% WO_3/Fe_2O_3	225–500 °C	~100%	600 ppm NH_3, 600 ppm NO, 5% O_2, 60,000 h^{-1}, 400 ml/min	[29]
0.05 ML WO_3/Fe_2O_3	300–550 °C	>90%	600 ppm NH_3, 600 ppm NO, 3% O_2, 72,000 h^{-1}, 600 ml/min	[58]
5 W/Fe_2O_3-AO-400	225–350 °C	>80%	600 ppm NH_3, 600 ppm NO, 5% O_2, 50,000 h^{-1}, 1000 ml/min	[59]
FW-GR/FW-SG	225–500 °C	>90%	600 ppm NH_3, 600 ppm NO, 5% O_2, 60,000 h^{-1}	[60]

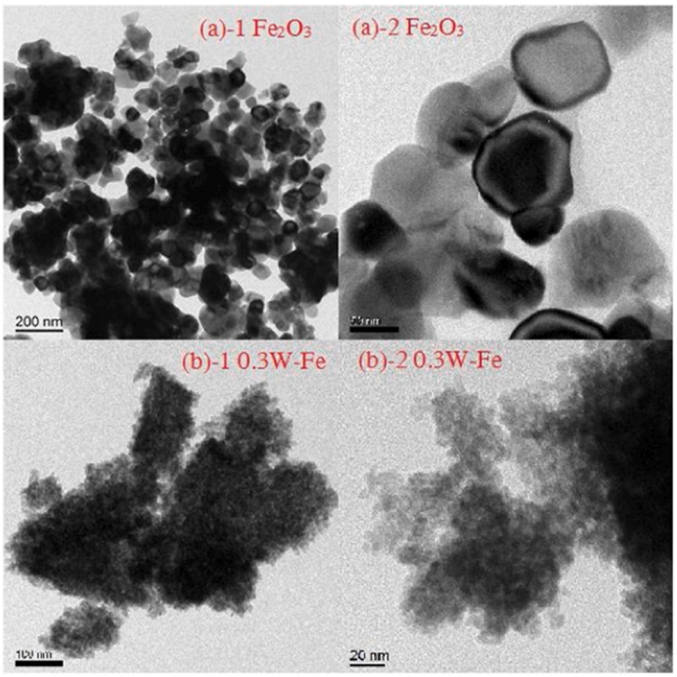

Fig. 4. TEM images of (a) pure Fe_2O_3 and (b) 0.3W-Fe catalysts [29].

et al. chose to reduce the active component of the catalyst to a monolayer thick entity to eliminate the particle shape effect, prepared a sub-monolayer WO_3 catalyst supported by Fe_2O_3, and determined the nature of the active center at the nanoscale [58]. The NO_x conversion rate of 0.05 monolayer (ML)WO_3/Fe_2O_3 catalyst is higher than 90% at 300–550 °C. The normalized SCR rate increased linearly with the square root of WO_3 coverage, and the amount of WO_3 in these catalysts was different, but the turnover number (TON) molar NO analysis results of 0.01, 0.03, and 0.05 ML WO_3/Fe_2O_3 were the same. This fact confirms that the active site is located at the interface between the WO_3 sub-monolayer and the carrier. The precise location of the active site can effectively reduce the waste of the W element. This is because the Fe-W catalysts have high SCR activity and wide temperature window at high temperatures, but low SCR activity. The magnetic 5 W/Fe_2O_3-AO-400 catalyst has a NO_x conversion rate of more than 80% at 225–350 °C, showing competitive low-temperature activity [59]. In addition to the interaction between W and Fe species, it is also found that tungsten doping can promote the collapse resistance of Fe_2O_3-AO pore structure, prevent γ-Fe_2O_3 from irreversibly turning into α-Fe_2O_3 during annealing at 400 °C, and effectively prevent the agglomeration and growth of Fe_2O_3 particles.

It is worth noting that the effects of preparation methods on the SCR activity of the Fe-W catalysts are summarized above. However, different reaction conditions in the preparation process will have a corresponding influence on the Fe-W catalyst, so it is of more reference value to reduce the uncertainty of variable factors and obtain the SCR activity of the Fe-W catalyst by different preparation methods. A series of Fe-tungsten (FW) composite oxide catalysts using different preparation methods, including the grinding (FW-GR), initial impregnation (FW-IM), sol-gel (FW-SG) and microemulsion methods (FW-ME) [60]. FW-GR and FW-SG catalysts achieved NO_x conversion rates above 90% at 225–500 °C (Fig. 5a). The denitrification performance of FW catalysts was mainly attributed to the presence of Fe^{2+} and $FeWO_4$ species on the surface, and more oxygen and $FeWO_4$ species were observed on the surface of FW-GR and FW-SG. In addition, in the actual working conditions of the NH_3-SCR catalyst, the temperature is an uncontrollable factor and has a large fluctuation, which will affect the surface acidity and defects of the catalyst. Therefore, it is necessary to study the effects of annealing temperature on the Fe-W catalyst. The surface defects and acidity of FW catalyst prepared by anhydrous grinding method were analyzed by changing the calcination temperature [61]. Fig. 5(b) shows the NH_3-SCR activity of Fe-W catalysts at different temperatures. The FW-400 °C catalyst has NO_x conversion rate of 90% at 213 °C and has the strongest low-temperature activity. The FW-500 °C catalyst exhibits an excellent T_{90} operating window in the 220–500 °C temperature range. With the increase in calcination temperature, the T_{90} operating window of the FW catalyst gradually narrowed. It is attributed to the decrease of BET surface area at high calcination temperature, corresponding to the reduced catalytic performance.

Based on the above analysis, the synergistic effects between W and Fe elements are mainly reflected in several aspects: (1) Increase the dispersion of transition metal oxides on the catalyst surface, making WO_x and FeO_x amorphous. (2) As a modifier, the W element can increase the surface acidity of the catalyst and have more acid sites and acid content. (3) The electron transfer between Fe and W facilitates the formation of Fe-O-W bonds, and can also properly adjust the redox capacity of the catalyst, thereby effectively inhibiting the non-selective oxidation of NH_3.

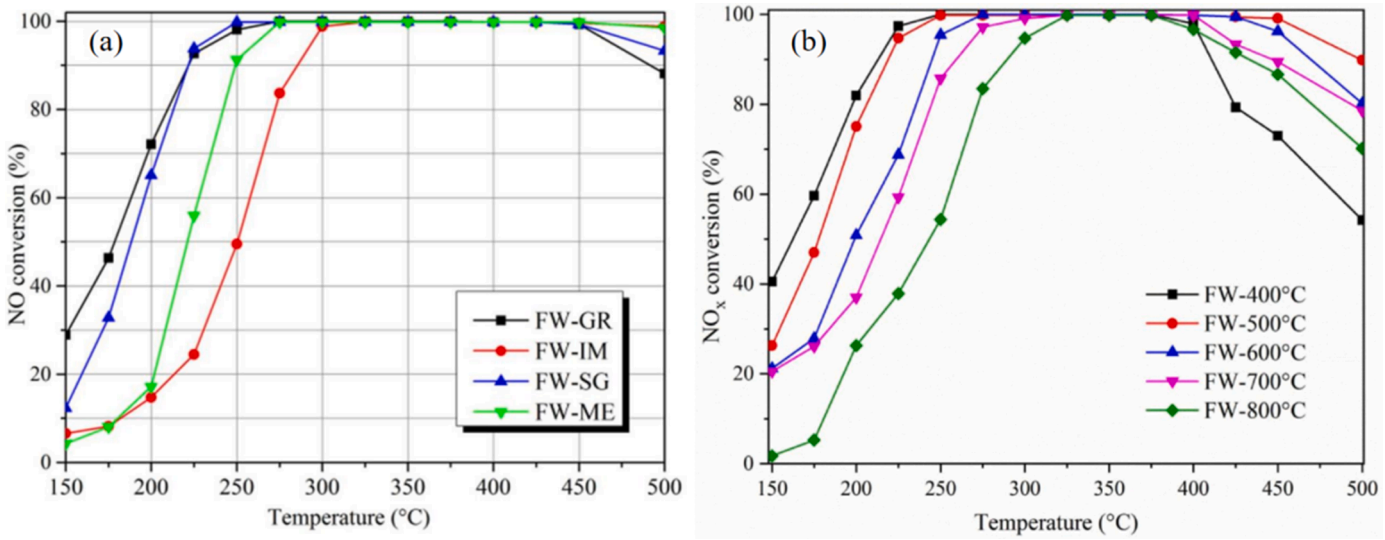

Fig. 5. NO and NO_x conversion of different FW catalysts: (a) NO; (b) NO_x at different temperatures [60,61].

3.1.3. Synergy between CeO_x and FeO_x

Ce element has excellent redox ability, good oxygen storage, and release ability, which can enhance the activation of chemisorbed NH_3 and the oxidation of NO during the NH_3-SCR process [62–64]. At the same time, the synergistic effect of environmentally friendly Ce-based oxide catalysts with other transition metal oxides can also effectively improve their redox capacity, thereby enhancing the NH_3-SCR activity of the catalysts [65]. The NH_3-SCR performance of different Fe-Ce catalysts is shown in Table 3.

For pure CeO_2, the addition of Fe_2O_3 could improve the redox capacity of the catalyst, but the enhancement of redox capacity did not improve the SCR activity of the catalyst, which was attributed to the lack of acidic sites on the surface [66]. Therefore, when CeO_x and FeO_x are selected as the active groups of catalysts, oxides with good acidity (such as Al_2O_3 or TiO_2) are usually selected as catalyst support to improve the SCR activity of catalysts. Using Al_2O_3 as catalyst support, $Ce_1Fe_{0.35}$ catalyst with a NO_x conversion rate exceeding 90% at 200–300 °C [67]. The excellent SCR activity was attributed to the replacement of Ce^{4+} (0.097 nm) by Fe^{3+}(0.064 nm) with a smaller ion radius in the synthesis process of the catalyst to form Ce-Fe solid solution. The NO conversion rate of the $3FeO_x$-$8CeO_2$/TiO_2 catalyst exceeds 98% in the 230–350 °C temperature range [68]. The interaction between Fe and Ce can promote the redox cycle on the catalyst ($Ce^{4+}+Fe^{2+}\Leftrightarrow Ce^{3+}+Fe^{3+}$). In addition, Ce doping increased the adsorption of NH_3 on the Lewis acid site of the catalyst and decreased the activation energy of the reaction. The NO conversion rate of Fe(0.2)-Ce(0.4)-Ti catalyst exceeded 94% in the 240–360 °C temperature range [69]. The synergistic effects of Fe and Ce species enhance the reverse process of redox equilibrium ($Ce^{4+}+Fe^{2+}\Leftrightarrow Ce^{3+}+Fe^{3+}$) and promote the formation of oxygen vacancies. In addition, in the presence of 200 ppm SO_2, the NO conversion rate of Fe (0.2)-Ce(0.4)-Ti catalyst still exceeds 92% within 25 h.

Ce-Fe catalyst has excellent SO_2 resistance, but we do not know the effect of the SO_2 presence on the active site of the Ce-Fe catalyst. The resistance of Ce-Fe/TiO_2/Al_2O_3 wire mesh honeycomb catalyst (Ce-Fe/WMH) at different concentration of SO_2 (100, 500, 1000 ppm) was tested at 250 ℃ [70]. As seen in Fig. 6(a), Ce-Fe/WMH catalyst showed good resistance to SO_2 poisoning within 100 h tested. The decrease in NO_x conversion during the first 50 min is the preferential adsorption of SO_2 to the Ce site, leading to the formation of sulfated cerium oxide on the catalyst surface. After 50 min, CeO_2 sulfation reached a stable state, and the NO_x decline trend slowed down. Interestingly, the incorporation of SO_2 into the Ce-Fe catalyst may lead to the formation of sulfate, resulting in a synergistic effect and improved SO_2 resistance of the Ce-Fe catalyst. Therefore, it is of great practical significance to directly sulfate the Ce-Fe catalyst to obtain the corresponding sulfate and analyze its influence on the surface acidity and redox performance of the Ce-Fe catalyst. The NO_x conversion rate of the 6FeSCe catalyst was greater than 90% between 300 °C and 450 °C [71]. After adding SO_2, the SCR activity of the 6FeSCe catalyst decreased very little, showing excellent sulfur resistance. There is a strong interaction between Fe, S, and Ce, so that electrons can be transferred from S to Ce^{4+} and Fe^{3+}, leading to an increase in the Ce^{3+} to Fe^{2+} ratio. Fe-S-Ce catalyst has a good SO_2 resistance and the NO_x conversion rate is close to 100% at 275–425 ℃. [72]. There is interfacial interaction between Fe, cerium oxide, and sulfate to form $Ce_2(SO_4)_3$ species on the Fe-S-Ce catalyst, which can effectively improve the surface acidity of the catalyst. Although the sulfation of the Fe-Ce catalyst effectively improved its SO_2 resistance and N_2 selectivity, the SCR activity at low temperature decreased compared with other non-sulfated Fe-Ce catalysts, and the temperature window shifted to the high-temperature region. Therefore, the presence of sulfate has a strong influence on the SCR activity of the Ce-Fe catalyst. It is of great value to further explore the influence of different preparation methods on the SCR activity of the Fe-S-Ce catalyst. Ce-Fe-O_x catalysts containing sulfate by the sol-gel (Fe-SG), hydrothermal (Fe-HT), co-precipitation (Fe-10), and solid-phase grinding synthesis methods (Fe-SSGS) [73]. As shown in Fig. 6(b), the Fe-HT catalyst has significantly higher NO_x conversion than other catalysts and exhibits 100% NO_x conversion at temperatures ranging from 250 °C to 450 °C. Appropriate sulfate species can promote the synergistic effect of Fe and Ce and improve the redox performance.

Due to extensive studies on the anti-SO_2 properties of Ce-Fe catalysts, the presence of $Ce_2(SO_4)_3$ species on the Ce-Fe catalysts may be attributed to the preference of SO_2 for adsorption to the Ce site. However, we do not know the adsorption process and decomposition process of sulfate on the catalyst surface. Therefore, to better develop the Ce-Fe catalyst, it is necessary to understand the adsorption mechanism of SO_2 on the Ce-Fe catalyst. The sulfur resistance of Ce-doped γ-Fe_2O_3 catalysts through quantum chemistry and density functional theory (DFT) and revealed the adsorption process of sulfur oxides on the catalyst surface and the decomposition process of surface sulfate [74]. The adsorption effect of Ce on SO_2 is much greater than Fe. The orbital coupling between Ce and SO_2 molecules occurs, and a large number of electrons enter the new bonding orbital. Thus, the addition of Ce can adsorb SO_2 molecules near the Ce cation, thus exposing more Fe active sites to air. In addition, the adsorption of SO_2 on the surface of the catalyst will form ammonium sulfate, and the doping of Ce will introduce more valence electrons, which will reduce the energy required for N—H bond breaking, and further reduce the activation energy required for sulfate decomposition.

In general, the synergy between Ce and Fe species is mainly reflected in the electron transfer capacity between Ce and Fe, which promotes the redox cycle ($Ce^{3+}+Fe^{3+}\Leftrightarrow Ce^{4+}+Fe^{2+}$), and then improves the redox capacity of the catalyst, which is consistent with the characteristics of the Ce-based catalyst. In addition, the interaction between Ce and Fe can inhibit the crystallization of CeO_x and FeO_x, improve the dispersion of metal oxides on the catalyst surface, adsorb more active species, and accelerate the NH_3-SCR reaction. The presence of Ce can effectively improve the SO_2 resistance and N_2 selectivity of the catalyst.

3.1.4. Synergy between VO_x and FeO_x

V-based catalysts have been widely used in commercial NH_3-SCR for

Table 3
NH_3-SCR activities of different Fe-Ce catalysts.

Catalyst	Temperature window	NO_x conversion	Reaction conditions	Refs.
CeO_2-Fe_2O_3	300 °C	74.68%	500 ppm NH_3, 500 ppm NO, 5% O_2, 75,000 h^{-1}, 1.25 L/min	[66]
Ce_1-$Fe_{0.35}$/Al_2O_3	200–300 °C	>90%	0.05% NH_3, 0.05% NO, 3% O_2, 6000 h^{-1}, 100 ml/min	[67]
$3FeO_x$-$8CeO_2$/TiO_2	230–350 °C	>98%	1000 ppm NH_3, 1000 ppm NO, 6% O_2, 30,000 h^{-1}	[68]
Fe(0.2)-Ce(0.4)-Ti	240–360 °C	>94%	500 ppm NH_3, 500 ppm NO, 5% O_2, 90,000 h^{-1}, 100 ml/min	[69]
Ce-Fe/WMH	250 °C	97.6%	1000 ppm NH_3, 1000 ppm NO, 3% O_2, 10,000 h^{-1}, 2000 ml/min	[70]
$6Fe_2(SO_4)_3$/CeO_2	300–450 °C	>90%	500 ppm NH_3, 500 ppm NO, 5% O_2, 118,000 h^{-1}, 300 ml/min	[71]
Fe-S-Ce	275–425 °C	~100%	600 ppm NH_3, 600 ppm NO, 5% O_2, 60,000 h^{-1}, 200 ml/min	[72]
Fe-HT	250–450 °C	100%	0.05% NH_3, 0.05% NO, 5% O_2, 100 ml/min	[73]

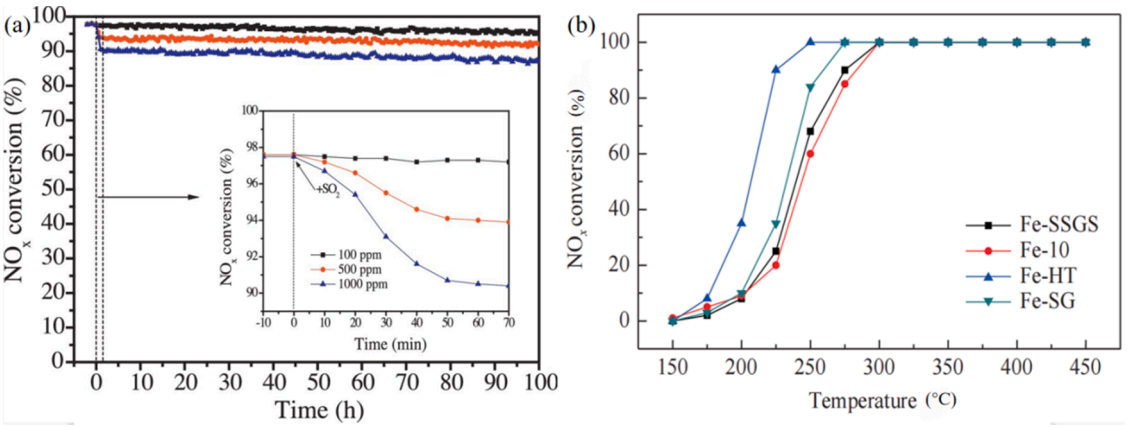

Fig. 6. NO_x conversion of different catalysts: (a) Effect of SO_2 on NO_x conversion of Ce-Fe/WMH catalyst; (b) NO_x conversion of Fe-SSGS, Fe-10, Fe-HT, and Fe-SG catalysts [70,73].

a long time, but some studies in recent years have found that it is being transferred to the low-temperature field [75]. Generally, V_2O_5 can be combined with other catalyst metal oxides, which can provide good Brønsted/Lewis acid sites and redox properties, and the interaction with other metal oxides can also improve the thermal stability and dispersion of the catalyst [76–78]. In recent years, the interaction between FeO_x and VO_x has been explored and used to promote the activity of SCR catalysts. The NH_3-SCR performance of different Fe-V catalysts is shown in Table 4.

It is well known that SCR performance and SO_2 resistance are often not superior when some low-cost natural minerals are used as catalyst raw materials. It is a good method to adjust the surface acidity and SO_2 resistance of catalysts by calcination and H_2SO_4 modification. A new mineral-derived catalyst (MDC) from vanadium titanomagnetite (VTM) and vanadium titanomagnetite sinter (VTMS) by calcination and sulfuric acid erosion modification [79]. After calcination, NO_x conversion on the VTM catalyst increased by 20–30%. The denitrification efficiency of the catalyst was also improved after sulfuric acid modification. Both VTM-A-5 and VTMS-A-5 catalysts showed about 90% NO_x conversion at 350 °C. The formation of sulfate species and the presence of $Fe^{3+}/Fe^{2+}$and V^{5+}/V^{4+} pairs in the catalyst effectively enhance the Brønsted acid site and redox performance of the catalyst. The SCR activity of the Fe-V catalyst can be improved by calcination and H_2SO_4 modification. However, the NO_x conversion rate is far from enough in the actual production process, so it is of great significance to improve the SCR activity of the Fe-V catalyst by new preparation methods. The NO_x conversion rate of $Fe_{0.75}V_{0.25}O_\delta$ catalyst prepared by urea homogeneous precipitation method is over 90% between 175 and 400 ℃[80]. The incorporation of V results in the formation of amorphous $FeVO_4$ and Fe_2O_3, amorphous phases with smaller particle sizes and higher oxygen mobility. The electron induction effect between Fe and V causes charge transfer from Fe to V, resulting in improved redox properties. In recent years, the research on TiO_2-supported Fe-V catalyst is increasing, because it is conducive to the dispersion of FeO_x and VO_x active substances. The NO_x conversion rate of the Fe_1-V_1/TiO_2 catalyst reached more than 90% at 220–420 °C [81]. The corresponding characteristic peaks of FeO_x and VO_x were not detected in the crystal phase structure of Fe-V oxide, and only the corresponding $FeVO_4$ peak was detected. The NO_x conversion rate of $Fe_{0.1}V_{0.1}TiO_x$ catalyst is more than 90% between 225 and 450 °C [82]. $FeVO_4$ and Fe_2O_3 species coexist and are highly dispersed on the TiO_2 surface, which enhances the electron transfer between Fe and V, resulting in charge imbalance.

For a long time, commercial V-based catalysts have been widely used for NO_x removal by the NH_3-SCR method. However, when used in diesel engine NO_x purification systems, the thermal stability at high temperatures and the resistance to SO_2 at low temperatures are relatively poor. The addition of Fe can effectively inhibit the volatilization of V_2O_5 and improve the resistance to SO_2. Therefore, it is of great significance to study the influence of Fe doping on the SCR performance of commercial V-based catalysts. With the increase of Fe_2O_3 content on the surface of Fe_2O_3-V_2O_5-WO_3/TiO_2 catalyst, the ratio of V^{4+}/V^{5+} decreases, and the oxidation rate of vanadium species SO_2 increases [83]. Three different catalysts by mechanically mixing V_2O_5-WO_3/TiO_2 and Fe_2O_3, including VW/Ti+Fe(N) by nano-replication, VW/Ti+Fe(P) by precipitation and VW/Ti+Fe(C) by using commercial Fe_2O_3 for comparison [84]. Fig. 7 shows the catalytic performance of VW/Ti and VW/Ti+Fe flowing with time at 275 °C in the presence of 600 ppm SO_2. Compared with the VW/Ti catalyst, the physical mixture of the VW/Ti+Fe catalyst showed better catalytic stability in the long-time reaction. As a greenhouse gas, N_2O has a single-molecule warming potential 298 times that of CO_2. It has been reported that the modification of V-based catalysts by Fe_2O_3 particles can significantly increase the strongly adsorbed NH_3 and NH_x components, which are involved in the reduction of N_2O formed at high temperatures, possibly due to the presence of Fe_2O_3-induced tetrahedrally coordination polymeric vanadates and surface V-O-Fe substances. [85]. They further found that the level of N_2O formation increased with the amount of V_2O_5 [86].

Therefore, it is clear that the combination of FeO_x and VO_x on the Fe-V catalysts can form $FeVO_4$ species, which can effectively improve the redox performance of the catalyst and provide more Brønsted/Lewis acid sites. In addition, the interaction between V and Fe species enhances the electron transfer ability between them, which is beneficial to obtain more Fe^{3+}, which in turn improves the NO_x conversion and N_2 selectivity of the catalyst.

Table 4
NH_3-SCR activities of different Fe-V catalysts.

Catalyst	Temperature window	NO_x conversion	Reaction conditions	Refs.
VTM-A-5/ VTMS-A-5	350 °C	~90%	300 ppm NH_3, 300 ppm NO, 6% O_2, 17,143 ml·$g^{-1}h^{-1}$, 1000 ml/min	[79]
$Fe_{0.75}V_{0.25}O_\delta$	175–400 °C	>90%	500 ppm NH_3, 500 ppm NO, 5% O_2, 50,000 h^{-1}, 200 ml/min	[80]
Fe_1-V_1/TiO_2	220–420 °C	>90%	0.05% NH_3, 0.05% NO, 5% O_2, 100,000 ml·$g^{-1}h^{-1}$, 500 ml/min	[81]
$Fe_{0.1}V_{0.1}TiO_x$	225–450 °C	>90%	500 ppm NH_3, 500 ppm NO, 5% O_2, 200,000 h^{-1}, 500 ml/min	[82]

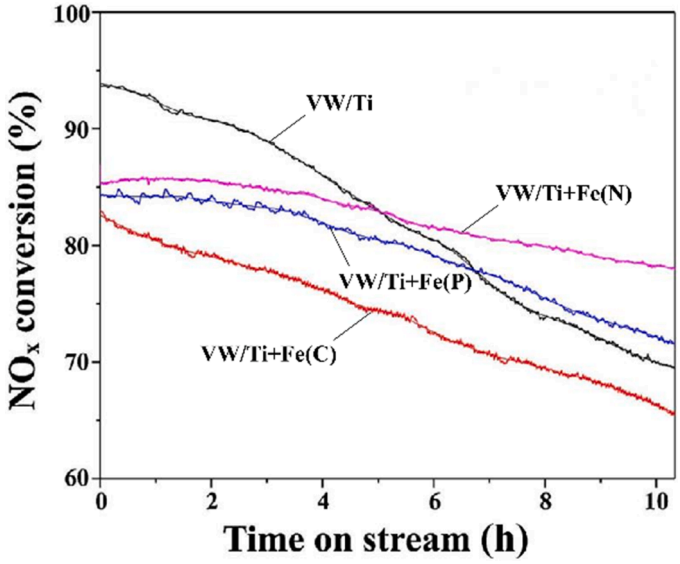

Fig. 7. NO_x conversion of VW/Ti and VW/Ti + Fe catalysts reacted at 275 °C for 10 h [84].

3.1.5. *Synergy between TiO_x and FeO_x*

As a semiconductor, TiO_2 can efficiently transfer electrons from TiO_2 to other metal elements and is considered to be a good additive [87,88]. Meanwhile, TiO_2, as a typical material with sufficient surface acidity, has been widely used in the development of commercial and novel catalyst supports. In addition, the introduction of Ti into other metals can modulate the interaction between metals and promote the adsorption of NO_x and NH_3, leading to charge imbalance, which in turn promotes the redox performance of the catalyst and improves surface acidity [89–91]. Table 5 shows the NH_3-SCR performance of different Fe-Ti catalysts.

The NO_x conversion rate of the γ-$Fe_{0.95}Ti_{0.05}O_z$ catalyst exceeded 90% between 250 and 400 °C [92]. It is found that the doping of Ti can reduce the grain diameter of the γ-Fe_2O_3 catalyst and refine the grain. γ-$Fe_{0.95}Ti_{0.05}O_z$ catalyst showed uniform spherical particle morphology, relatively independent between particles without adhesion, and pore connectivity was good. To further analyze the influence of the presence of Ti^{4+} on the electronic structure of γ-Fe_2O_3 and the changes in the redox behavior and acidity of the catalyst, doped Ti^{4+} into γ-Fe_2O_3, and found that Ti^{4+} occupied the octahedral vacancy, replacing part of the octahedral iron site, and the interaction between high Ti^{4+} ions and O^{2-} [101]. Thus, the entropy of spinel is reduced and the stability of γ-Fe_2O_3 is effectively improved. The NO_x conversion rate of the $Fe_9Ti_1O_x$ catalyst is more than 80% at 150–350 °C [93]. It was found that Ti^{4+} promoted the formation of Fe-O-Ti species, which improved the redox properties of Fe_2O_3, and Ti^{4+} doping enhanced the surface acidity of the catalyst.

In recent years, by optimizing the surface structure and morphology of TiO_2, the BET surface area of the catalyst was improved and an effective mass transfer channel was formed, to adsorb and activate more reactive gasses. The NO_x conversion rate of the Fe/TNT (titanium dioxide nanotubes) catalyst is greater than 80% between 200 and 350 °C [94]. TiO_2 in the Fe/TNT catalyst is transformed into an amorphous tubular structure of $H_2Ti_3O_7$. At present, direct preparation of FeTi catalyst by the template method is also effective. Template modification can also effectively regulate the physical and chemical properties and structure of the FeTi catalyst. FeTi(f), FeTi(c) and FeTi(p) catalysts were synthesized using an additive polymer of polypropylene glycol (F127), cetyltrimethylammonium bromide (CTAB) and polyethylene glycol (PEG) as templates, respectively [95]. As shown in Fig. 8, the SCR performance of FeTi catalyst prepared by the template method is much better than pure FeTi catalyst, and the NO_x conversion rate of the FeTi(c) catalyst exceeds 90% between 180 and 360 °C. This is because the smallest particle of FeTi(c) is only 12 nm, which has a large specific surface area. The morphology and structure of TiO_2 was modified and synthesized Fe/Ti@Si catalysts with higher specific surface area, amorphous structure along mesoporous channels, and more acidic sites than Fe/TiO_2 [96]. Thin layer of TiO_2 is easier to absorb electrons from the supported Fe_2O_3 than the bulk TiO_2, which promotes the

Table 5
NH_3-SCR activities of different Fe-Ti catalysts.

Catalyst	Temperature window	NO_x conversion	Reaction conditions	Refs.
γ-$Fe_{0.95}Ti_{0.05}O_z$	250–400 °C	>90%	0.1% NH_3, 0.1% NO, 3.5% O_2, 30,000 h^{-1}, 3000 ml/min	[92]
$Fe_9Ti_1O_x$	150–350 °C	>80%	500 ppm NH_3, 500 ppm NO, 5% O_2, 60,000 h^{-1}, 100 ml/min	[93]
Fe/TNT	200–350 °C	>80%	1000 ppm NH_3, 900 ppm NO, 100 ppm NO_2, 10% O_2, 50,000 h^{-1}	[94]
FeTi(c)	180–360 °C	>90%	500 ppm NH_3, 500 ppm NO, 6.5% O_2, 12,000 h^{-1}, 400 ml/min	[95]
Fe/Ti@Si	275–400 °C	>80%	500 ppm NH_3, 500 ppm NO, 5% O_2, 75,000 ml·$g^{-1}h^{-1}$, 200 ml/min	[96]
$FeTiSO_x$-2.0	300–500 °C	>90%	800 ppm NH_3, 800 ppm NO, 3% O_2, 80,000 h^{-1}	[97]
Fe-Ti-MMT	350–420 °C	~100%	500 ppm NH_3, 500 ppm NO, 5% O_2, 38,000 h^{-1}	[98]
$Ti_{0.1}Sm_{0.075}Fe_{0.085}O_x$	150–300 °C	>90%	650 ppm NH_3, 650 ppm NO, 6% O_2, 15,000 h^{-1}, 100 ml/min	[99]
7.5%Ti-$Fe_xMg_yO_z$	225–400 °C	100%	0.1% NH_3, 0.1% NO, 3.5% O_2, 30,000 h^{-1}, 2 L/min	[100]

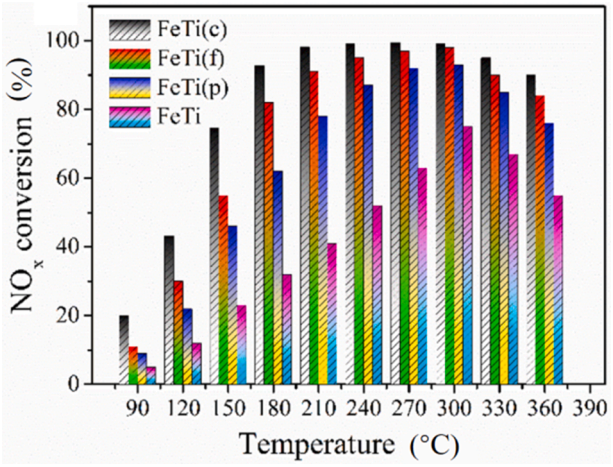

Fig. 8. NO_x conversion of FeTi catalysts [95].

enhancement of Fe-O-Ti interface interaction, leading to the redox performance improvement of the catalyst and acidity enhancement.

To ensure the surface acidity of the FeTi catalyst, a modified FeTi catalyst with sulfate species was proposed. The new $FeTiSO_x$-2.0 catalyst showed a NO_x conversion rate of over 90% at 300–500 °C [97]. The linked hydroxyl group of the sulfate material and the Ti^{4+} on the surface can effectively form the Brønsted acid site. The formation of Fe-O-Ti and Fe-O-S species can also significantly enhance the acidic site of the catalyst. It is well known that the SCR activity of catalysts can be seriously affected by alkali/heavy metal poisoning in addition to better SO_2 resistance. In fact, because of the coexistence of alkali and heavy metals in practical applications, the lifetime of catalysts is severely inhibited. To solve this problem, synthesized a Fe-Ti-montmorillonite (MMT) catalyst, which had almost 100% NO conversion rate at the 350–420 °C temperature window [98]. After alkali/heavy metal co-poisoning, the inactivation rate of NO conversion was about 10%, showing excellent alkali and heavy metal resistance. As seen in Fig. 9, the Fe-Ti-MMT catalyst shows an obvious stratified structure, which is attributed to the natural form of MMT. After alkali/heavy metal co-poisoning, several particles are observed on the layer surface, which are K and Pb substances partially deposited on the surface of the Fe-Ti-MMT catalyst. The incorporation of Ti can effectively inhibit the attack of the Fe active site by K or Pb, and maintain a high reduction capacity to the poisoned Fe-Ti-MMT catalyst.

At present, the modification of Fe polyoxide based on TiO_2 has been widely studied. As an excellent additive, titanium can widely improve the redox properties and surface acidity of Fe-based catalysts. The NO_x conversion rate of titanium-modified $Ti_{0.1}Sm_{0.075}Fe_{0.825}O_x$ catalyst was over 90% at 150–300 °C [99]. The 7.5% Ti-$Fe_xMg_yO_z$ catalyst can achieve 100% NO_x conversion at 225–400 °C [100]. The doping of Ti plays the following roles: (1) To provide more acidic sites; (2) Improved BET surface area of catalyst; (3) TiO_x and FeO_x exist as an amorphous phase in the catalyst to form a good solid solution; (4) It changes the electron cloud density of other elements and affects the interactions between different species. Therefore, the introduction of Ti helps to broaden the temperature range of the NH_3-SCR reaction.

3.1.6. *Synergy between ZrO_x and FeO_x*

ZrO_2 is a good semiconducting transition metal oxide with excellent hydrothermal stability at high temperatures [102]. The addition of ZrO_2 as a promoter to other metal oxides can effectively adjust the surface acidity of the catalyst and reduce the concentration of basic sites, thereby improving the resistance of the catalyst to SO_2 poisoning [103,104]. Through the strong interaction between ZrO_2 and other metal oxides, ZrO_2 can also enhance the redox performance and oxygen storage capacity of catalysts, inhibit the crystallization of metal oxides and improve their dispersion [105,106]. The NH_3-SCR performance of different Fe-Zr catalysts is listed in Table 6.

The synergistic effects between Fe and Zr are due to the ionic radius of Zr^{4+} in ZrO_2 (0.086 nm) being larger than Fe^{3+} in Fe_2O_3 (0.069 nm) [112]. Some Zr^{4+} ions may be replaced by Fe^{3+} to form Fe_2O_3-ZrO_2 solid solution in a lattice position. In addition, the synergistic effect also promoted the redox reaction ($Fe^{3+}+Zr^{3+}\Leftrightarrow Fe^{2+}+Zr^{4+}$). Some studies have suggested that the enhanced SCR performance of the Fe-Zr catalyst caused by the introduction of SO_2 may be due to the enhanced acidity of sulfated ZrO_2 support. Compared with the Fe/Zr catalyst, the activity of the Fe/(SZr) sulfated iron-based catalyst was significantly increased at 250–500 °C and the NO_x conversion rate reached more than 90% at 300–450 °C [107]. The presence of sulfate, Fe_2O_3, and SO_4^{2-} species on the Fe/(SZr) catalyst provides more acid sites. The NO_x conversion rate of the Fe_2SZr catalyst reached more than 90% at 350–450 °C [108]. Fe^{3+} has a strong adsorption capacity of NO_x and NH_3 species at medium-low temperatures, but the increase of Fe^{3+} at high temperatures will promote the oxidation of NH_3. The addition of SO_4^{2-} will reduce the redox activity of the catalyst, resulting in the reduction of SCR activity at medium and low temperatures, but will inhibit the oxidation of NH_3 at high temperatures. Thus, the appropriate ratio of redox sites (Fe^{3+}) and acid sites (SO_4^{2-}) yields high SCR activity. ZrO_2 is also used as an additive to improve the catalytic activity of catalysts based on their acidity. The Zr-modified ferric samarium oxide catalyst showed that the addition of Zr increased the weak acid site but decreased the medium acid site [99]. The NO_x conversion rate of the novel Fe^{3+} and Zr^{4+} co-doped $CeTiO_x$ catalyst was higher than 80% between 250 and 400 ℃ [109]. The co-doping of Fe^{3+} and Zr^{4+} can inhibit the agglomeration of Fe and the grain size growth of the catalyst, and improve the redox capacity and surface acidity of the catalyst. In addition, the co-doping of Fe^{3+} and Zr^{4+} inhibited grain growth during the secondary calcination process.

In recent years, metallic columnar montmorillonite (PILM) has been widely studied as an acid carrier with a high specific surface area and adjustable rich surface acidity. The interaction of ZrO_2 and Fe_2O_3 in Zr-Fe polymer-supported sandwich montmorillonite (Zr-Fe-PILM) inhibits the crystallinity of ZrO_2 and $Fe2O_3$, and increases the BET surface area of the catalyst [113,114]. The same results also appeared on the ZrO_2--supported sulfated Fe_2O_3 catalyst (FeS/Zr) [110]. No α-Fe_2O_3 or $Fe_2(SO_4)_3$ diffraction reflections were observed because of the ZrO_2 presence. However, the BET specific surface area of pure ZrO_2 support is only 4.53 m^2/g, which has a great influence on the SCR activity of the

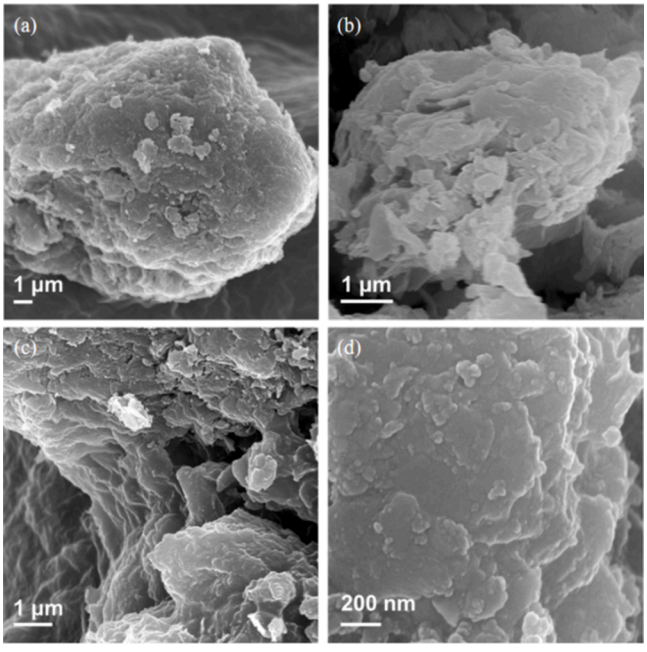

Fig. 9. SEM images of (a) Fe-MMT-E, (b) Fe-MMT, (c) Fe-Ti-MMT, and (d) K/Pb-Fe-Ti-MMT catalysts [98].

Table 6
NH_3-SCR activities of different Fe-Zr catalysts.

Catalyst	Temperature window	NO_x conversion	Reaction conditions	Refs.
Fe/(SZr)	300–450 °C	>90%	500 ppm NH_3, 500 ppm NO, 3% O_2, 47,000 h^{-1}, 300 ml/min	[107]
Fe_2SZr	350–450 °C	>90%	500 ppm NH_3, 500 ppm NO, 3% O_2	[108]
FZCT	250–400 °C	>80%	500 ppm NH_3, 500 ppm NO, 5% O_2, 60,000 h^{-1}, 200 ml/min	[109]
FeS/Zr	350–450 °C	>80%	500 ppm NH_3, 500 ppm NO, 3% O_2, 47,000 h^{-1}, 300 ml/min	[110]
3%Fe/WO_3-ZrO_2	400–550 °C	80–85%	100 ppm NH_3, 100 ppm NO, 12% O_2, 5% CO_2, 10% H_2O, 2 L/min	[111]

catalyst. Therefore, as a carrier with high stability and excellent surface acidity, ZrO_2 is often doped with other elements to effectively improve the physical and chemical properties of the ZrO_2 carrier. The 3wt% Fe/WO_3-ZrO_2 catalyst achieved 80–85% NO_x conversion in the 400–550 °C temperature range [111]. Due to the strong interaction between Fe-ZrO_2, Fe would preferentially interact with the free Zr^{4+} site to generate more Lewis sites. In addition, the key function of Fe is to convert Lewis acid sites into reaction sites.

In conclusion, the strong interaction between Zr and Fe will not only improve the redox performance of the catalyst but also enhance the number and strength of catalyst acid sites, thereby enhancing the adsorption capacity of the Fe-Zr catalyst for NH_3 and NO_x species. At the same time, the presence of ZrO_2 can also effectively inhibit the crystallization of Fe_2O_3 and improve its dispersion on the catalyst. All these factors contribute to the high NH_3-SCR activity of the Fe-Zr catalysts.

3.1.7. Synergy between other metal oxides and Fe oxides

In recent years, to improve the SCR activity of Fe-based catalysts, some other metals (Ho, Mg, Co, Al, Nb, Mo, etc.) have also been widely used for doping. It is generally believed that the unique interaction between different elements often produces different effects on the catalyst. The NH_3-SCR performance characteristics of Fe-based catalysts modified with different elements are listed in Table 7.

As a rare earth metal, Ho has incomplete 4*f* and empty 5*d* orbitals. The surface of Ho_2O_3 has different Lewis acid sites (Ho^{3+}) [128]. The NO_x conversion rate of $Fe_{0.3}Ho_{0.1}Mn_{0.4}/TiO_2$ catalyst is higher than 85% at 60–200 °C [115]. The doped Ho_2O_3 can improve the dispersion of the Fe_2O_3 phase to the greatest extent and maintain the amorphous phase, and generate new Lewis acid sites. In addition, the effects of SO_2 on the SCR activity of $Fe_{0.3}Ho_{0.1}Mn_{0.4}/TiO_2$ catalysts at low temperatures were investigated [129]. After the introduction of SO_2, the SCR activity of the catalyst decreased sharply, mainly due to the deposition of ammonium sulfate and ammonium bisulfate on the catalyst surface and the formation of $MnSO_4$. After thermal reduction and regeneration of the catalyst, it was found that the catalytic activity of the catalyst could not be fully recovered. It was found that $MnSO_4$ could not be reduced completely, and some S element still existed in the catalyst. On the other hand, the catalyst particles agglomerate, and $(NH_4)_2SO_4$ sediment clogs the pore structure.

As an alkaline earth metal, Mg tends to reduce the interaction between elements at low temperatures, thus inhibiting the activity of NH_3-SCR. However, it has also been found that although the addition of Mg has some adverse effects on the physical and chemical characteristics of the catalyst, Mg can interact with other metal oxides to form solid solutions, thus promoting the SCR activity and stability of the catalyst [130]. The NO_x conversion rate of the $Fe_{0.8}Mg_{0.2}O_z$ catalyst exceeded 90% between 250 and 350 °C [116]. Mg can refine the γ-Fe_2O_3 microcrystals and produce strong interaction with iron oxide to form a solid solution, and also make the specific surface area of γ-Fe_2O_3 increases sharply. In addition, the lower the calcination temperature was, the better SCR activity was [131]. Different calcination temperatures can affect the interaction between different species by changing the electron cloud density and electron affinity potential. The lower the calcination temperature, the better the synergistic interaction between Fe, Mg, and O.

Co has variable valence, and its oxide has excellent oxygen storage capacity. Co-doping can effectively increase the amount of catalyst acid, resulting in a large number of Brønsted acid sites, which is conducive to NH_3 adsorption [132]. The NO conversion rate of the Co-FeO_x catalyst is close to 100% at 170–290 °C [117]. The Co doping into α-Fe_2O_3 leads to the formation of $CoFe_2O_4$ crystal, and increases the relative amount of Fe^{3+} and surface oxygen in the Co-FeO_x catalyst. So far, carbon-based materials have been widely studied due to their high BET surface area and adsorption capacity. NO conversion of Co-Fe_2O_3/AC catalyst is about 90% between 200 ℃ and 240 °C [118]. CoO_x can be uniformly dispersed on the catalyst surface or exist as an amorphous oxide on the surface. To further understand the synergistic effects between Fe and Co, based on Fe and Co elements, the improvement of Hg^0 removal and SO_2 resistance of catalysts by Fe and Co co-doping was also studied. The 2Fe4Co-MCT catalyst showed a better performance in removing NO and Hg^0 at the same time, and the NO_x conversion rate was about 90% at 150–250 °C [119]. The introduction of Fe species enhanced the SCR activity, and the introduction of Co species enhanced Hg^0 oxidation. The synergistic effects of Fe and Co species played an important role in the simultaneous removal of NO and Hg^0. The NO conversion rate of the 2Fe4Co-MCT catalyst was close to 100% at 125–250 °C [120]. After adding 200 ppm SO_2, the SCR activity of the 2Fe4Co-MCT catalyst could remain above 96% after about 7 h. Fe and Co co-doping can effectively reduce the adsorption of SO_2 and prevent the diffusion of SO_2 into the inner layer of the catalyst.

Al_2O_3 has good mechanical properties and thermal stability. At the

Table 7
NH_3-SCR activities of iron-based catalysts modified with different elements.

Catalyst	Temperature window	NO_x conversion	Reaction conditions	Refs.
$Fe_{0.3}Ho_{0.1}Mn_{0.4}/TiO_2$	60–200 °C	>85%	0.08% NH_3, 0.08% NO, 5% O_2, 20,000 h^{-1}, 100 ml/min	[115]
$Fe_{0.8}Mg_{0.2}O_z$	250–350 °C	>90%	0.1% NH_3, 0.1% NO, 3.5% O_2, 30,000 h^{-1}, 2 L/min	[116]
Co-FeO_x	170–290 °C	~100%	500 ppm NH_3, 500 ppm NO, 3% O_2, 42,000 h^{-1}, 200 ml/min	[117]
Co-Fe_2O_3/AC	200–240 °C	~90%	500 ppm NH_3, 500 ppm NO, 5% O_2, 100 ml/min	[118]
2Fe4Co-MCT	150–250 °C	~90%	500 ppm NH_3, 500 ppm NO, 3% O_2, 30,000 h^{-1}, 1500 ml/min	[119]
2Fe4Co-MCT	125–250 °C	~100%	500 ppm NH_3, 500 ppm NO, 6% O_2, 12,000 h^{-1}, 400 ml/min	[120]
$Fe_{1.2}Al_{0.8}O_x$	250–350 °C	>80%	800 mg·m^{-3} NH_3, 800 mg·m^{-3} NO, 6% O_2, 300 ml/min	[121]
Fe-Mn/Ce_1Al_2	75–250 °C	>90%	500 ppm NH_3, 500 ppm NO, 5% O_2, 30,000 h^{-1}	[122]
$Nb_{30.3}FeO_x$	250–400 °C	~100%	500 ppm NH_3, 500 ppm NO, 5.3% O_2, 50,000 h^{-1}, 300 ml/min	[123]
$FeNb_{0.4}O_x$-C	250–400 °C	>90%	500 ppm NH_3, 500 ppm NO, 5% O_2, 250,000 h^{-1}, 500 ml/min	[124, 125]
$Fe_{0.94}Sm_{0.06}O_x$	175–325 °C	>95%	0.05% NH_3, 0.05% NO, 5% O_2, 60,000 h^{-1}	[126]
$Fe_4Mo_1O_x$	250–450 °C	>90%	500 ppm NH_3, 500 ppm NO, 5% O_2, 50,000 h^{-1}, 500 ml/min	[127]
Mo-Fe_2O_3	300–400 °C	>90%	0.1% NH_3, 0.1% NO, 3.5% O_2, 30,000 h^{-1}, 2 L/min	[37]

same time, as a catalyst modifier, it can improve the dispersion of metal oxides and provide rich acidic sites to enhance the adsorption ability of the catalyst to NH_3 species [133,134]. The NO conversion rate of the $Fe_{1.2}Al_{0.8}O_x$ catalyst was higher than 80% at 250–350 °C [121]. Compared with AlO_x and FeO_x, $Fe_{1.2}Al_{0.8}O_x$ has a better NO conversion rate. This was attributed to the synergistic interaction and uniform distribution between Fe and Al, which increased the moderately acidic sites on the catalyst. Li et al. also noticed that Al doping made Fe species have better dispersion on the catalyst surface, and could effectively increase the number and strength of acidic sites on the catalyst surface [122].

Niobium oxide itself has a high acid strength. The introduction of Nb can enhance the surface acidity of the catalyst and improve the dispersion of metal oxides [135]. The $Nb_{30.3}FeO_x$ catalyst showed a NO_x conversion rate of nearly 100% at 250–400 °C [123]. The presence of the Nb element leads to the appearance of a new phase, $FeNbO_4$, and the lattice parameters of the Fe_2O_3 phase are reduced due to the replacement of Fe ions (0.0645 nm) by smaller Nb ions (0.064 nm). The NO_x conversion rate of the $FeNb_{0.4}O_x$-C catalyst exceeded 90% at 250–400 °C [124,125]. The strong interaction between Fe and Nb promotes the formation of the γ-Fe_2O_3 active phase. This interaction provides more active sites for the $FeNb_{0.4}O_x$-C catalyst.

Sm_2O_3 is a kind of rare earth metal oxide with good thermal stability, sufficient redox properties and oxygen storage/release capacity. The addition of Sm species can significantly increase the acidic sites of the catalyst, effectively enhance the adsorption of oxygen on the catalyst surface, and promote the oxidation of NO [136]. The NO_x conversion rate of the $Fe_{0.94}Sm_{0.06}O_x$ catalyst is greater than 95% at 175–325 °C [126]. The synergistic interaction between Fe and Sm improves the electron distribution of Fe and Sm atoms, leading to the reverse process of redox reactions ($Fe^{3+}+Sm^{2+}\Leftrightarrow Fe^{2+}+Sm^{3+}$), which favors the oxidation of NO and NH_3. In addition, the number of weak and medium strong acid sites on the catalyst surface was significantly increased by the appropriate amount of Sm doping.

In recent years, Mo has been widely used as a catalyst for the NH_3-SCR catalysts. The interaction between Mo and Fe can enhance the surface acidity and the number of active sites [137]. The NO conversion rate of the $Fe_4Mo_1O_x$ catalyst was greater than 90% at 250–450 °C [127]. There is a synergistic effect between Fe and Mo species, which can reduce the crystal size of Fe_2O_3 and increase the surface acidity of the catalyst. Mo is widely used in SCR reactions because of its typical arsenic resistance. Arsenic preferentially combines with active iron sites on γ-Fe_2O_3 catalyst and significantly consumes the surface Lewis/Brønsted acid sites, resulting in the inhibition of the reaction of coordination ammonia and gaseous NO_x on γ-Fe_2O_3 [37]. The introduction of Mo can effectively prevent the binding of active iron sites to gaseous arsenic. In addition, the interaction between Mo and Fe destroys the crystal structure of MoO_3 and Fe_2O_3 magnetite phase, forming the amorphous -O-Mo-O-Fe-O- structure.

In summary, it was found that the interaction between other metal oxides and FeO_x can effectively improve the redox characteristics and surface acidity of the catalyst, thereby better adsorbing NH_x and NO_x species, improving the NH_3-SCR activity of the catalyst. The addition of some metal oxides can also improve the dispersion and stability of FeO_x on the catalyst surface.

3.1.8. Synergy between multi-component Fe-based oxide catalysts

The synergistic effects between the three elements can better improve the redox properties, surface acidity, BET surface area, surface dispersion, and SO_2 resistance of the catalyst [138–140]. On the one hand, a double redox cycle may be formed between the three elements, accelerating electron transfer and promoting the generation of oxygen vacancies. On the other hand, each element plays a different role in improving the performance of the catalyst, thereby improving the performance of the catalyst in all aspects. The NH_3-SCR performance characteristics of the multicomponent Fe-based catalysts are listed in Table 8.

Table 8
NH_3-SCR activity of multicomponent Fe-based catalysts.

Catalyst	Temperature window	NO_x conversion	Reaction conditions	Refs.
$Fe_{0.3}Mn_{0.5}Zr_{0.2}$	200–360 °C	100%	500 ppm NH_3, 500 ppm NO, 4% O_2, 35,000 h^{-1}, 500 ml/min	[141]
FMZ-(400, 500, 600 °C)	170–360 °C	100%	500 ppm NH_3, 500 ppm NO, 4% O_2, 35,000 h^{-1}, 500 ml/min	[142]
Ce(12.5)-$FeMNO_x$	90–135 °C	>97%	0.1% NH_3, 0.1% NO, 3% O_2, 30,000 h^{-1}, 860 ml/min	[143]
3%Mn1%Ce-siderite	180–300 °C	>90%	0.05% NH_3, 0.05% NO, 3% O_2, 10,000 h^{-1}, 1.5 L/min	[47]
Mn-Fe-Ce	175–300 °C	>80%	500 ppm NH_3, 500 ppm NO, 11% O_2, 36,000 h^{-1}, 300 ml/min	[144]
MnFeW/Ti	140–250 °C	>80%	500 ppm NH_3, 500 ppm NO, 5% O_2, 80,000 h^{-1}, 1 L/min	[40]
Fe-W-Ce	210–500 °C	>90%	450 ppm NH_3, 450 ppm NO, 2.5% O_2, 20,000 h^{-1}	[145]
$Fe_{0.65}Ce_{0.05}Ti_{0.30}O_z$–MH	150–400 °C	>90%	0.1% NH_3, 0.1% NO, 3% O_2, 30,000 h^{-1}, 3000 ml/min	[146]
FeNbTi	200–270 °C	>80%	500 ppm NH_3, 500 ppm NO, 4% O_2, 24,000 h^{-1}	[147]
FeS/(Ti_1Zr_4)	300–500 °C	>90%	500 ppm NH_3, 500 ppm NO, 3% O_2, 47,000 h^{-1}, 300 ml/min	[110]

Due to the excellent activity of Fe-based catalysts at medium and high temperatures and insufficient activity at low temperatures, the most common method is to use Mn element doping to improve the SCR activity of Fe-based catalysts at low temperatures. Therefore, based on the Fe-Mn catalyst, adding other elements to enhance the physical and chemical characteristics of the catalyst has been widely studied. The NO conversion rate of the $Fe_{0.3}Mn_{0.5}Zr_{0.2}$ catalyst was 100% between 200 and 360 °C. The $Fe_{0.3}Mn_{0.5}Zr_{0.2}$ catalyst has excellent texture capacity, and a BET-specific surface area of 309 m^2/g, which can provide more active sites [141]. In addition, the interaction of Fe, Mn and Zr, which leads to the increase of Zr-O coordination bond length, and the improvement of surface acidity and alkalinity, which promotes the electron transfer on the catalyst surface. The Fe-Mn-Zr catalyst prepared

by changing the calcination temperature (T = 400, 500, 600, 700, 800 °C) can achieve 100% NO removal efficiency in the range of 170–360 °C when calcined at 400–600 °C [142]. The low calcination temperature is beneficial to the high dispersion of FeOx and MnO_x on the surface of ZrO_2. Moreover, due to the good thermal stability of ZrO_2 itself, the interaction between ZrO_2 and MnO_x, and FeO_x also leads to the change of the acidity of the catalyst surface, which ultimately affects the adsorption performance of the catalyst surface to the active substances.

In recent years, to improve the SCR activity and SO_2 resistance of Fe-Mn catalysts, CeO_2 as a low-content modifier has been widely used in catalytic applications. The Ce(12.5)-$FeMnO_x$ catalyst had a NO_x conversion rate of more than 97% between 90 °C and 135 °C [143]. By partially blocking the adsorption site, ceria changes the local surface structure of the catalyst and changes the amount of oxygen adsorbed on the surface. The NO_x conversion rate of the 3%Mn1%Ce-siderite catalyst is greater than 90% between 180 and 300 °C [47]. Mn and Ce co-doping can increase BET surface area and surface acidity of siderite. The electron transfer and interaction of Fe, Mn and Ce elements improved the SCR activity of the catalyst. As shown in Fig. 10, the SCR activity of Fe-Mn-Ce catalyst is much higher than pure Ce and Mn-Ce samples [144]. The interaction between them promotes the generation of more oxygen vacancies and improves the surface acidity and reducibility of the catalyst.

The synergistic interaction between Fe and W, the redox properties and surface acidity of the catalyst can be effectively improved. Therefore, the development of new multi-element catalysts based on Fe-W catalysts has obvious advantages. The NO_x conversion rate of the MnFeW/Ti catalyst was higher than 80% between 140 and 250 °C [40]. Mn, Fe, and W interact with each other and have their effects. As the main active species, Mn exhibits strong acid and redox properties. Fe species can promote the dispersion of MnO_x species and provide more acidic sites for reactant adsorption and activation. The W species can change the surface structure of the MnFeW/Ti catalyst and form Mn-O-W and Fe-O-W bonds, leading to the dispersion of surfactant and easy transport of electrons and oxygen. The NO_x conversion rate of the $Fe_{0.5}$-W-Ce catalyst is greater than 90% between 210 and 500 °C [145]. The synergistic effects of Fe, W, and Ce effectively inhibit the crystallization of metal oxides. The SCR performance of multi-element catalysts can also be improved by changing the preparation method. The $Fe_{0.65}Ce_{0.05}Ti_{0.30}O_z$–MH catalyst by microwave hydrothermal co-precipitation, which showed higher SCR activity than $Fe_{0.65}Ce_{0.05}Ti_{0.30}O_z$ in the low-temperature range of 125–175 °C [146]. Microwave hydrothermal treatment can enhance the interaction between Fe, Ce, and Ti, accelerate the microcrystalline rate of Fe, Ce and Ti mixed oxide catalyst precursor, and increase the pore size and pore volume of the catalyst.

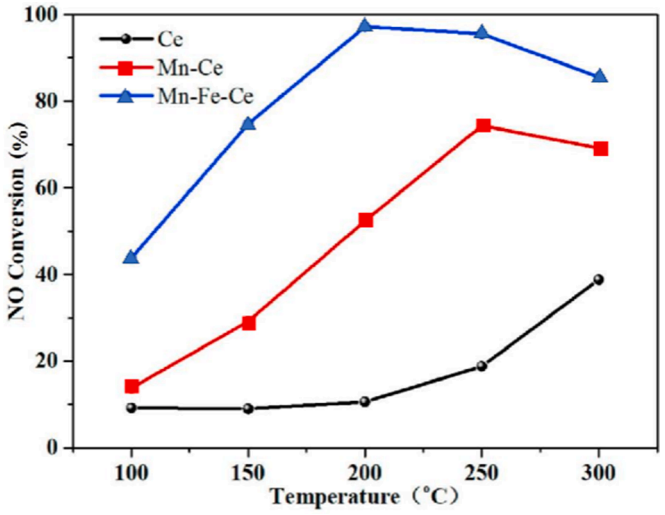

Fig. 10. NO conversion of Ce, Mn-Ce, and Fe-Mn-Ce catalysts [144].

In practical industrial applications, catalysts are often accompanied by a large amount of SO_2, which will lead to the poisoning of the active site of catalysts and deactivation. Therefore, green and environmentally friendly catalysts attract a large number of researchers at home and abroad. The catalyst is often accompanied by a large amount of SO_2 in practical industrial applications, the active site of the catalyst will be poisoned and deactivated. Therefore, the research how to realize green and environmentally friendly catalysis has attracted a large number of scientists. Fig. 11(a) shows environmentally-friendly FeNbTi catalysts with different Nb doping [147]. The catalytic activity of the FeNbTi catalyst prepared by Nb (0.03, 0.05) doping is better than the FeTi and NbTi catalysts. The high activity may be due to the maximum synergistic effects among Nb, Fe, and Ti species, which will promote the high dispersion of Nb_2O_5 and Fe_2O_3 in the FeNbTi catalyst. As seen in Fig. 11 (b), adding different concentrations of SO_2 from 100 ppm to 400 ppm had negligible effects on the FeNb(0.05)Ti catalyst, and the NO conversion rate exceeded 90% at 250 °C. However, the activity of the FeTi catalyst has been decreasing, and the higher the concentration of SO_2, the lower the activity of the catalyst. This shows that the FeTi catalyst modified by niobium has strong resistance to SO_2 poisoning. The NO_x conversion rate of the FeS/(Ti_1Zr_4) catalyst is greater than 90% at 300–500 °C, and the NO_x conversion rate of FeS/(Ti_1Zr_4) is greater than 96% after feeding SO_2 at 300 °C, which lasts for 14 h in the presence of SO_2, showing excellent SO_2 resistance [110].

In conclusion, based on the multi-element doped composite oxide catalysts, rational doping can tune the synergy between metal ions and promote electron transfer between different elements, thereby effectively improving the redox properties and surface acidity of the catalyst. In addition, the synergistic effects between different elements help to improve the SO_2 and H_2O tolerance of the catalyst, which can effectively suppress the deactivation of the active sites on the catalyst surface, opening a new path for the development of catalysts with high SCR activity and high SO_2 tolerance for practical industrial applications.

3.2. *Nonmetallic elements-modified Fe-based catalyst*

It is generally believed that the improvement of catalyst acidity is beneficial to the adsorption of NH_3 to improve the SCR activity of the catalyst, and the modification of SCR catalysts with phosphates, sulfates, and heteropolyacids is an effective method to improve the surface acidity [148–150]. The NH_3-SCR performance characteristics of different non-metal-modified Fe-based catalysts are listed in Table 9.

3.2.1. *Effects of heteropoly acid modification on Fe-based oxide catalysts*

The versatility of heteropoly acid compounds as catalysts has attracted extensive attention. Heteropoly acids are highly stable and easy to synthesize. They are often used as acid catalysts and oxidation catalysts and have been proven to be of great value in basic research and practical applications [159–161]. In addition, heteropoly acid has excellent surface acidity and redox properties, and its addition can change the molecular properties of the catalyst, enhance the electron transfer at the metal-oxide interface in the catalyst, and the strength and site density of the acid, thereby promoting the SCR activity of the catalyst [162–164].

Keggin-structured phosphotungstic acid ($H_3PW_{12}O_{40}$, HPW) and phosphorus tungstate are typical heteropoly compounds, which have been widely used to modify NH_3-SCR catalysts. A new HPW-modified annular Fe_2O_3 catalyst with NO_x conversion higher than 90% at 250–500 °C [151].The synergistic interaction between Fe species and HPW polyanion can increase the surface acidity and acid sites, and improve the thermal stability of HPW polyanion. The NO_x conversion rate of tungsten-phosphate (TPA) modified Fe_2O_3 nanocycles (TPA/-Fe_2O_3) is above 92% in 230–500 °C [152]. There is some interaction between the terminal oxygen of TPA and Fe^{3+} of Fe_2O_3, which leads to

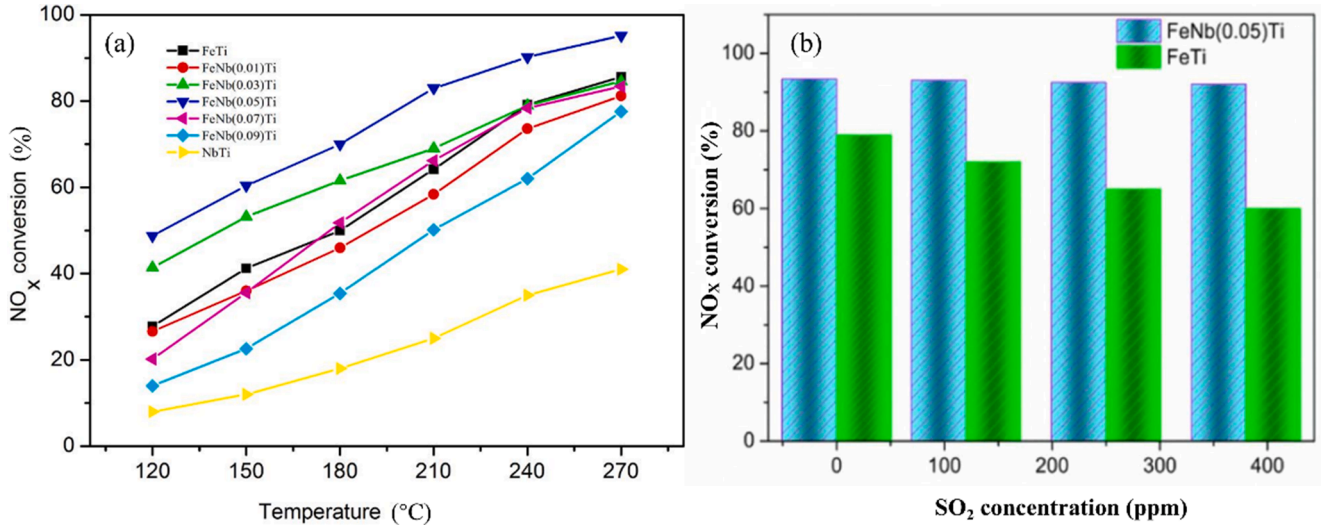

Fig. 11. (a) SCR activity on FeTi, NbTi and FeNbTi catalysts with different Nb doping; (b) Effects of different SO_2 concentrations on FeTi and FeNb(0.05)Ti catalysts [147].

Table 9
NH_3-SCR activities of Fe-based catalysts modified with different non-metallic elements.

Catalyst	Temperature window	NO_x conversion	Reaction conditions	Refs.
MCG-HPW/Fe_2O_3 NRs	250–500 °C	>90%	1100 ppm NH_3, 1000 ppm NO, 6% O_2, 13,200 h^{-1}, 100 ml/min	[151]
TPA/Fe_2O_3	230–500 °C	>92%	1100 ppm NH_3, 1000 ppm NO, 6% O_2, 13,200 h^{-1}, 100 ml/min	[152]
HPW/Fe_2O_3–500	200–400 °C	>90%	500 ppm NH_3, 500 ppm NO, 5% O_2, 30,000 $cm^3g^{-1}h^{-1}$, 100 ml/min	[30]
HPW/Fe_2O_3–350–0.5	240–460 °C	~100%	500 ppm NH_3, 500 ppm NO, 5% O_2, 14,400 h^{-1}	[153]
SO_4^{2-}/$Fe(OH)_3$	250–450 °C	>80%	0.06% NH_3, 0.06% NO, 5% O_2, 60,000 h^{-1}, 400 ml/min	[154]
Ce/Fe-Zr-0.3S	250–450 °C	>80%	0.08% NH_3, 0.08% NO, 5% O_2, 60,000 h^{-1}, 400 ml/min	[155]
Sulfated CeFe	250–450 °C	>80%	1000 ppm NH_3, 1000 ppm NO, 4% O_2, 45,000 h^{-1}, 300 ml/min	[156]
FTP1.5	200–400 °C	>80%	500 ppm NH_3, 500 ppm NO, 3% O_2, 60,000 h^{-1}	[157]
$Fe_{0.3}Ce_{0.7}$	240–390 °C	>95%	500 ppm NH_3, 500 ppm NO, 5% O_2, 60,000 h^{-1}, 150 ml/min	[31]
$Fe_{0.2}W_{0.2}Ti$ ($U_{0.03}$)	1240–420 °C	>95%	500 ppm NH_3, 500 ppm NO, 5% O_2, 25,000 h^{-1}	[158]

the enhancement of acid strength and redox performance of the TPA/-Fe_2O_3 catalyst, which is similar to the previous modification of HPW. The NO_x conversion rate of HPW/Fe_2O_3–500 is higher than 85% at 250–500 °C in the presence of SO_2 and H_2O [30]. During the calcination of HPW/Fe_2O_3, the ferrous cation on magnetite is oxidized by O_2 to form the edge of maghemite. The iron oxide in HPW/Fe_2O_3–500 mainly exists in the form of Fe_3O_4. The graft of HPW prevents the outward migration of ferrous ions and inhibits the recrystallization of Fe_2O_3. The modification of HPW can greatly improve the resistance of catalysts to SO_2. However, the effects of HPW modification on the NH_3-SCR reaction of Fe_2O_3 catalysts in the presence of SO_2 and the corresponding resistance mechanism of SO_2 are still unclear. The NO_x conversion rate of the HPW/Fe_2O_3–350–0.5 catalyst is close to 100% at 240–460 °C [153]. When 100 ppm SO_2 was added, the HPW/Fe_2O_3–350–0.5 catalytic activity decreased from 100% to 70.3% in 1 h, and then gradually recovered to close to 100% in the following 5 h. On the contrary, the catalytic activity of the Fe_2O_3–350 catalyst decreased significantly when SO_2 was introduced, and the conversion rate of NO decreased to 40% within 6 h. The SCR reaction is mainly attributed to Fe_2O_3–350 catalyst through the L-H mechanism. In the presence of SO_2, SO_2 and NO will compete and adsorb on the active site, thus blocking the active site and destroying the redox cycle of Fe^{3+}/Fe^{2+} and inhibiting the L-H reaction pathway. The HPW/Fe_2O_3–350–0.5 catalyst followed the E-R mechanism, effectively inhibited the adsorption and oxidation of NO/SO_2, and thus effectively improved the resistance of SO_2.

3.2.2. *Effects of sulfuric acid modification on Fe-based oxide catalysts*

Sulfuric acid-modified metal oxide catalysts have been extensively studied in recent years [165–167]. In particular, the modification of sulfuric acid often increases the strength and number of Brønsted/Lewis acid sites on the catalyst, adsorbs more NH_3 species, and inhibits the oxidation of NH_3, showing excellent NH_3-SCR catalytic activity and H_2O+SO_2 resistance [165,166]. In addition, the catalysts modified by sulfuric acid also show good redox performance and improve the low-temperature activity of the catalysts [167].

The NO_x conversion rate of the SO_4^{2-}/$Fe(OH)_3$ catalyst is over 80% at 250–450 °C, and it has good resistance to H_2O+SO_2 [154]. The functionalization of sulfuric acid can inhibit the growth of Fe_2O_3 grains. SO_4^{2-} and Fe^{3+} can combine to form a sulfate complex, leading to an increase in the number and strength of acidic sites on the surface. Due to the improvement of SCR performance of FeO_x catalyst by sulfuric acid modification, the research on multi-element catalysts based on sulfuric

acid modification has been increasing. The NO_x removal rate of the Ce/Fe-Zr-0.3S catalyst was higher than 80% at 250–450 °C [155]. Sulfuric acid treatment of Ce/Fe-Zr can increase surface acidity and produce more active sites, and increase the interaction between the elements and thus induce a synergistic interaction between acidity and redox on the catalyst. To further understand the synergistic interaction between sulfuric acid modification and multi-element catalyst and electron transfer, sulfate-modified mesoporous Fe-doped CeO_2 catalyst, and the NO_x conversion rate exceeded 80% at 250–450 °C [156]. The organic-like sulfuric acid base group bound to Fe-O-Ce material results in strong electronic interaction between Fe^{3+}-O-Ce^{4+} and the sulfuric acid base group, which changes the acidity and redox properties of the catalyst. In addition, the presence of metal sulfate species perturbs the electron interactions and redox cycles of Fe and Ce, breaking the Fe-O-Ce bonds.

3.2.3. Modifications by other non-metal elements

As far as we know, some other non-metallic elements modified multi-component catalysts can also change the physical and chemical properties of the main active components to effectively improve the SCR activity of the catalyst. For example, phosphorus-containing compounds in typical toxic flue gas emissions, often combine with catalyst active sites during the release process, resulting in catalyst deactivation [168]. However, due to the acidity of phosphorus itself, phosphorus poisoning may increase the acidity of the catalyst surface, thereby promoting the SCR reaction of the catalyst.

Compared with the $FeTiO_x$ catalyst, the addition of phosphorus decreased the SCR activity at low temperatures but enhanced the SCR activity at high temperatures [157]. Phosphorus interacts with Ti and Fe atoms to form P-O-Fe and P-O-Ti structures, which block Lewis acid sites. However, the presence of phosphate also provides additional Brønsted acid sites (P-O-NH_4^+), which opens a new reaction pathway for them to participate in high-temperature reactions. To more intuitively solve the interface existing in the active site after phosphorus doping, the NO_x conversion of the new Fe-doped $CePO_4$ ($Fe_{0.3}Ce_{0.7}$) catalyst was greater than 95% between 240 and 390 ℃ [31]. Phosphate in the Fe_x-Ce_{1-x} catalyst is the active site for effective adsorption and activation of NH_3 species. The NO_x conversion rate of the urea-modified $Fe_{0.2}W_{0.2}Ti$ ($U_{0.03}$) catalyst was over 95% at 240–420 °C [158]. The addition of urea not only increases the dispersion of Fe and W but also decreases the crystallinity of titanium. In addition, the presence of urea also significantly increased the acid adsorption site, reducibility, and adsorption oxygen concentration of the catalyst.

In summary, although the modification of non-metallic elements will block the active site of the catalyst and lead to the reduction of SCR activity, it can also produce synergistic interaction with FeO_x, or promote the synergistic interaction among multiple elements, to effectively improve the redox characteristics and surface acidity of the catalyst. This modification may change the reaction pathway of the catalyst and the active sites involved in the reaction, leading to further improvements in the SCR activity and SO_2 resistance. Therefore, this work on the modification of non-metallic elements also provides a new avenue for the development of future NH_3-SCR catalysts.

4. Effects of unique morphology on Fe-based catalysts

In the process of SCR reaction, the gas involved in the reaction needs to diffuse to the surface of the inner pore of the catalyst, adsorb and activate, and then the product gas involved in the reaction is diffused and discharged from the pores. Therefore, some porous or macro-porous structures can effectively reduce the diffusion resistance of gas in the catalyst and provide more active sites due to their high BET surface area, thus reducing the activation energy required for the reaction, accelerating the mass transfer and diffusion of gas, and thus effectively improving the SCR activity of the catalyst [169–171]. Table 10 shows the NH_3-SCR performance of Fe-based catalysts with different morphology.

Table 10
NH_3-SCR activities of Fe-based catalysts with different morphology.

Catalyst	Temperature window	NO_x conversion	Reaction conditions	Refs.
3DOM $Ce_{0.7}Fe_{0.2}Ti_{0.1}O_2$	281–425 °C	100%	1000 ppm NH_3, 1000 ppm NO, 3% O_2, 100,000 h^{-1}, 100 ml/min	[172]
3DOM $Fe_{9.0}V_{1.0}$	220–412 °C	>80%	500 ppm NH_3, 500 ppm NO, 5% O_2, 60,000 $ml{\cdot}g^{-1}h^{-1}$, 100 ml/min	[173]
Ce@Ce-Fe	295–480 °C	>80%	500 ppm NH_3, 500 ppm NO, 5% O_2, 30,000 h^{-1}	[174]
$MnFeO_x$@TiO_2	180–400 °C	>90%	600 ppm NH_3, 600 ppm NO, 5% O_2, 108,000 h^{-1}	[175]
FMTs	150–360 °C	>90%	500 ppm NH_3, 500 ppm NO, 5% O_2, 40,000 h^{-1}, 200 ml/min	[176]
Fe_2O_3@MnO_x@CNTs	120–300 °C	>90%	550 ppm NH_3, 550 ppm NO, 5% O_2, 20,000 h^{-1}	[177]
Fe_2O_3–2S	225–325 °C	100%	0.1% NH_3, 0.1% NO, 4% O_2, 30,000 h^{-1}, 2 L/min	[178]
MnO_x-FeO_x	120–240 °C	100%	500 ppm NH_3, 500 ppm NO, 5% O_2, 36,000 h^{-1}, 600 cm^3/min	[39]
MnFeCo-LDO	50–400 °C	>86%	500 ppm NH_3, 500 ppm NO, 5% O_2, 30,600 h^{-1}, 100 ml/min	[179]

4.1. Effect of 3DOM structure on Fe-based oxide catalysts

In recent years, three-dimensional ordered macroporous (3DOM) structures have been widely used for NO_x removal by the NH_3-SCR method. Due to its periodic ordered and interconnected macroporous structure, it can provide mass transfer channels for the reaction gas to enter the internal active sites, and has a high specific surface area and more active sites, which is beneficial to the SCR reaction [180–182]. In addition, soot, as a typical emission particulate matter, has low combustion efficiency on the catalyst surface due to its size being larger than 25 nm. Therefore, the macro-porous structure of 3DOM facilitates the transfer and diffusion of PM in the inner pores.

A novel 3DOM $Ce_{0.7}Fe_{0.2}Ti_{0.1}O_2$ catalyst has a 100% NO_x conversion between 281 and 425 ℃, and the maximum CO_2 concentration of soot (PM) combustion is at 385 °C [172]. The double redox cycle among the three elements ($Fe^{3+}+Ce^{3+}\Leftrightarrow Fe^{2+}+Ce^{4+}$, $Fe^{3+}+Ti^{3+}\Leftrightarrow Fe^{2+}+Ti^{4+}$) and the synergistic effect of Fe, Ti, and Ce promote the high catalytic performance of the catalyst. In addition, as shown in Fig. 12(a), the 3DOM structure has an ordered and interconnected macropore structure, which is conducive to providing more channels for adsorption and reaction species and facilitating their transfer and diffusion on the inner pore, and PM can also enter the inner pore (Fig. 12(b)). As seen in Fig. 13, the NO_x conversion rate of the traditional $Fe_{9.0}V_{1.0}$ catalyst in the absence of soot is greater than 80% at 244–394 °C and the NO_x conversion rate of

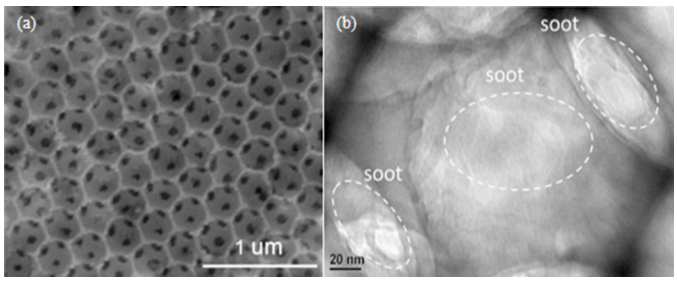

Fig. 12. SEM image of (a) 3DOM $Ce_{0.7}Fe_{0.2}Ti_{0.1}O_2$ material; (b) 3DOM $Ce_{0.7}Fe_{0.2}Ti_{0.1}O_2$ catalyst mixed with soot [172].

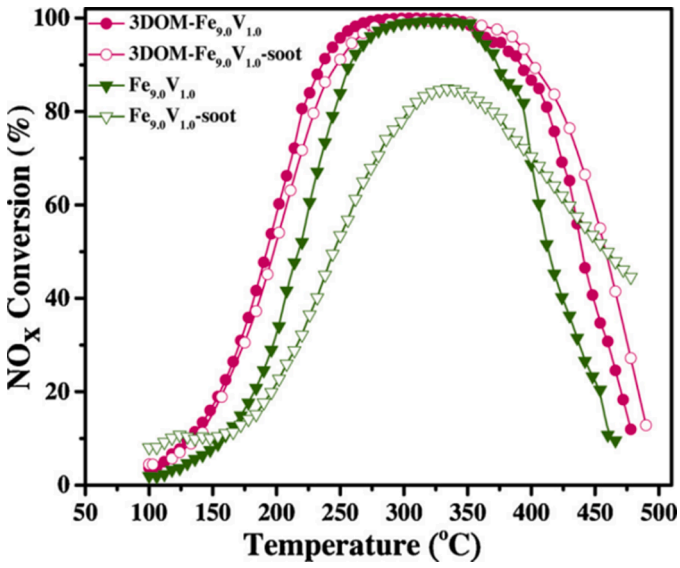

Fig. 13. NO_x conversion as a function of temperature after exposure of catalyst loosely mixed with model soot particles [173].

the 3DOM-$Fe_{9.0}V_{1.0}$ catalyst is more than 80% at 220–412 °C [173]. In the presence of soot, the NO_x conversion rate of the traditional $Fe_{9.0}V_{1.0}$ catalyst decreases, and the activity of the 3DOM-$Fe_{9.0}V_{1.0}$ catalyst decreases slightly. The NO_x conversion rate is greater than 80% at 230–420 °C. The high SCR activity of 3DOM materials can be attributed to the dust trapped in the large pores of 3DOM, which weakens or inhibits the dust coverage effects on the catalyst surface, and finally exposes more active sites.

4.2. Effect of core-shell structure on Fe-based oxide catalysts

Due to its unique structural characteristics, the core-shell structure wraps a layer of metal oxide on the active components of the core, thereby improving the stability and dispersion of the core. In addition, the two different properties of the inner and outer layers complement their respective deficiencies, which is an important research direction in which the morphology determines the catalyst activity in recent years.

The Ce@Ce-Fe Prussian blue analog had a NO_x conversion rate of more than 80% between 295 °C and 480 °C [174]. As shown in Fig. 14 (a), the Ce@Ce-Fe catalyst has a typical biconical structure with uniform size and structure and the same particle size. The selected-area electron diffraction (SAED) patterns in Fig. 14(b) have three diffraction rings indicating that Ce@Ce-Fe is polymorphic. The well-defined pore with uniform diameter in Ce@Ce-Fe (Fig. 14(c)) confirms its mesoporous structure, which facilitates the dispersion of active components and the exposure of more active sites. Therefore, the unique morphological and mesoporous structure features provide a larger specific surface area and more active sites for the adsorption and activation of reactive gasses. So far, it has been found that the core-shell structure can also effectively prevent other pollutants (SO_2, K, etc.) in the exhaust gas from contacting the active site and causing the deactivation of the catalyst. A core-shell $MnFeO_x@TiO_2$ catalyst with a NO_x conversion rate of more than 90% at 180–400 °C and showed excellent K tolerance [175]. The interaction between Mn, Fe, and Ti in the core-shell structure was found to be strong, and the $MnFeO_x@TiO_2$ catalyst showed excellent surface acidity. On the other hand, the core-shell structure of the $MnFeO_x@TiO_2$ catalyst can improve its reducibility and contribute to redox cycling in SCR reactions. As seen in Fig. 15, Mn and Fe species are mainly covered by TiO_2 shells, while K species are attached to their outer surfaces. Therefore, the existence of the core-shell structure of the $MnFeO_x@TiO_2$ catalyst can effectively protect the active species of catalyst from K poisoning, and inhibit the aggregation phenomenon of the catalyst due to K poisoning. Li et al. prepared a $MnO_x@Fe_2O_3$ core-shell catalyst (FMTs) by loading metal oxides on titanium dioxide nanotubes (TNT) [176]. The excellent performance of core-shell FMTs is mainly attributed to the interfacial confinement characteristics of Fe_2O_3 and the proper regulation of the structure of TNTs on the strong component interaction and oxidation performance of MnO_x. It is also found that the Fe_2O_3 shell can limit the sulfurization of MnO_x particles by SO_2. Moreover, the nano-domain limiting effect of TiO_2 nanotubes can regulate the oxidation ability of metal oxides to a certain extent.

In recent years, the improved SCR activity and SO_2 resistance of Fe-based catalysts by monolayer core-shell structure proved the feasibility of the core-shell structure. Researchers were inspired to prepare Fe-based catalysts with the multi-shell structure to obtain high SCR activity and SO_2 resistance. A multi-shell $Fe_2O_3@MnO_x@CNTs$ catalyst with NO_x conversion greater than 90% at 120–300 °C[177]. The results show that the Fe@Mn@CNT multi-shell structure can greatly improve the SCR activity of the catalyst and enhance the surface-reducible species. As shown in Fig. 16, Fe species are mainly located in the outer layer of the nanocomposite, while the Mn signal appears in the middle layer and the C signal can only be observed inside the catalyst. This fully indicates that the wrapped Fe_2O_3 can be used as a protective layer to protect the inner MnO_x and inhibit the deactivation of SO_2 by the catalyst. In short, the existence of this core-shell structure can form a protective layer to block the contact between some toxic components and active components,

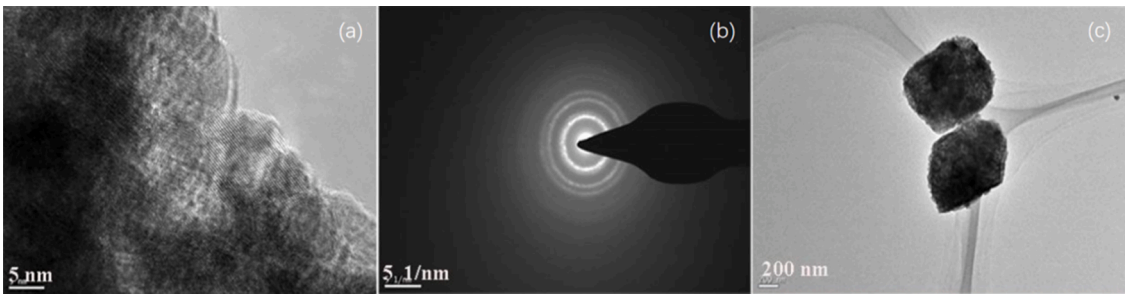

Fig. 14. (a) TEM image of Ce@Ce-Fe; (b) selected-area electron-diffraction pattern (SAED); (c) typical low-magnification TEM image [174].

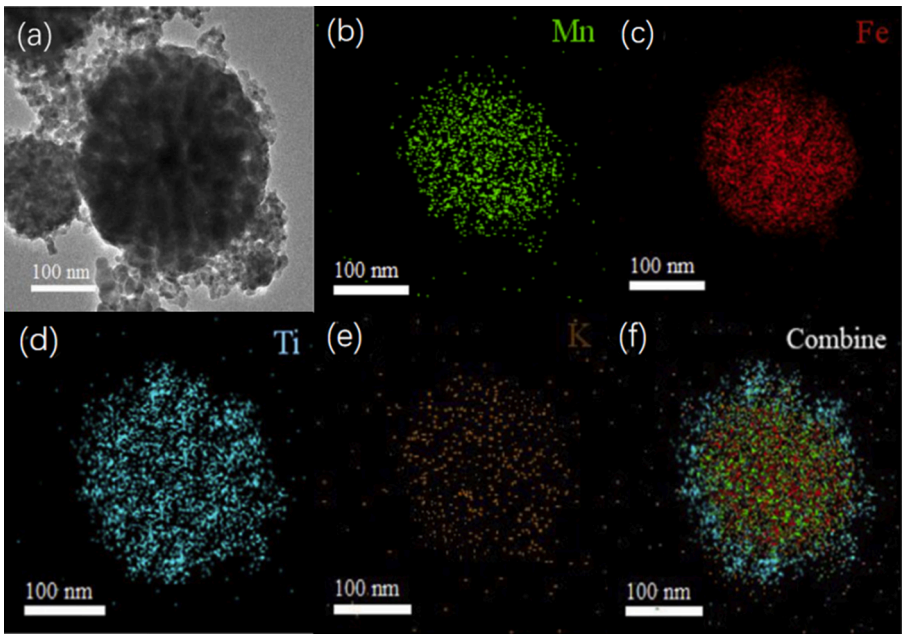

Fig. 15. TEM image of (a) $MnFeO_x$@TiO_2-K. The corresponding elemental maps analysis of the $MnFeO_x$@TiO_2-K sample showing (b) Mn, (c) Fe, (d) Ti, (e) K, and (f) Combined element distribution maps [175].

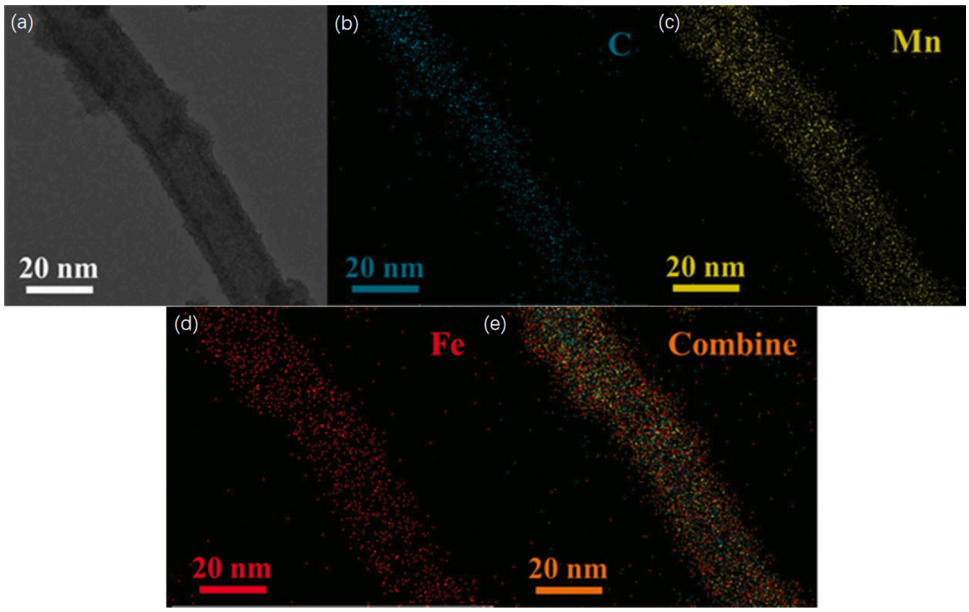

Fig. 16. HAADF-STEM image of (a) Fe@Mn@CNTs. The corresponding elemental maps of the Fe@Mn@CNTs sample showing (b) C, (c) Mn, (e) Fe, and (f) Combined elements distribution maps [177].

thus protecting the activity of the catalyst. This typical core-shell structure can also effectively inhibit the aggregation of active components and enhance the high dispersion of active components, thus promoting the increase of active sites.

4.3. Influence of porous/multilayer structure on Fe-based oxide catalysts

Generally speaking, some porous or multilayer SCR catalysts can provide a large BET surface area, lower diffusion resistance and have more gas mass transfer channels, which is beneficial to the catalytic performance of the catalyst. Metal-organic frames (MOFs) are typically porous materials with layered pore systems and large BET areas [32].

MIL-100(Fe) was used as a template to prepare a new porous α-Fe_2O_3 nanocatalyst (Fe_2O_3–2S) with 100% NO_x conversion at 225–325 °C [178]. As shown in Fig. 17, Fe_2O_3–2S retains the original morphology structure of the precursor, which has more tunnel structure. This morphology has two types of mesopore, which can provide a more specific surface area, meaning that the Fe_2O_3–2S catalyst has more active sites. A novel porous nanometer needle-like MnO_x—FeOx catalyst was developed. MnO_x—FeO_x nanoneedles have 100% NO_x conversion at 120–240 °C [39]. Compared with MnO_x—FeO_x nanoparticles, MnO_x—FeO_x nanoneedles have higher BET surface area, stronger acidic sites, and higher reduction properties due to their unique porous nanoneedle structure and uniform distribution of O, Mn, and Fe on the surface. The layered structure has a unique two-dimensional structure with high dispersion and more active sites. The two-dimensional

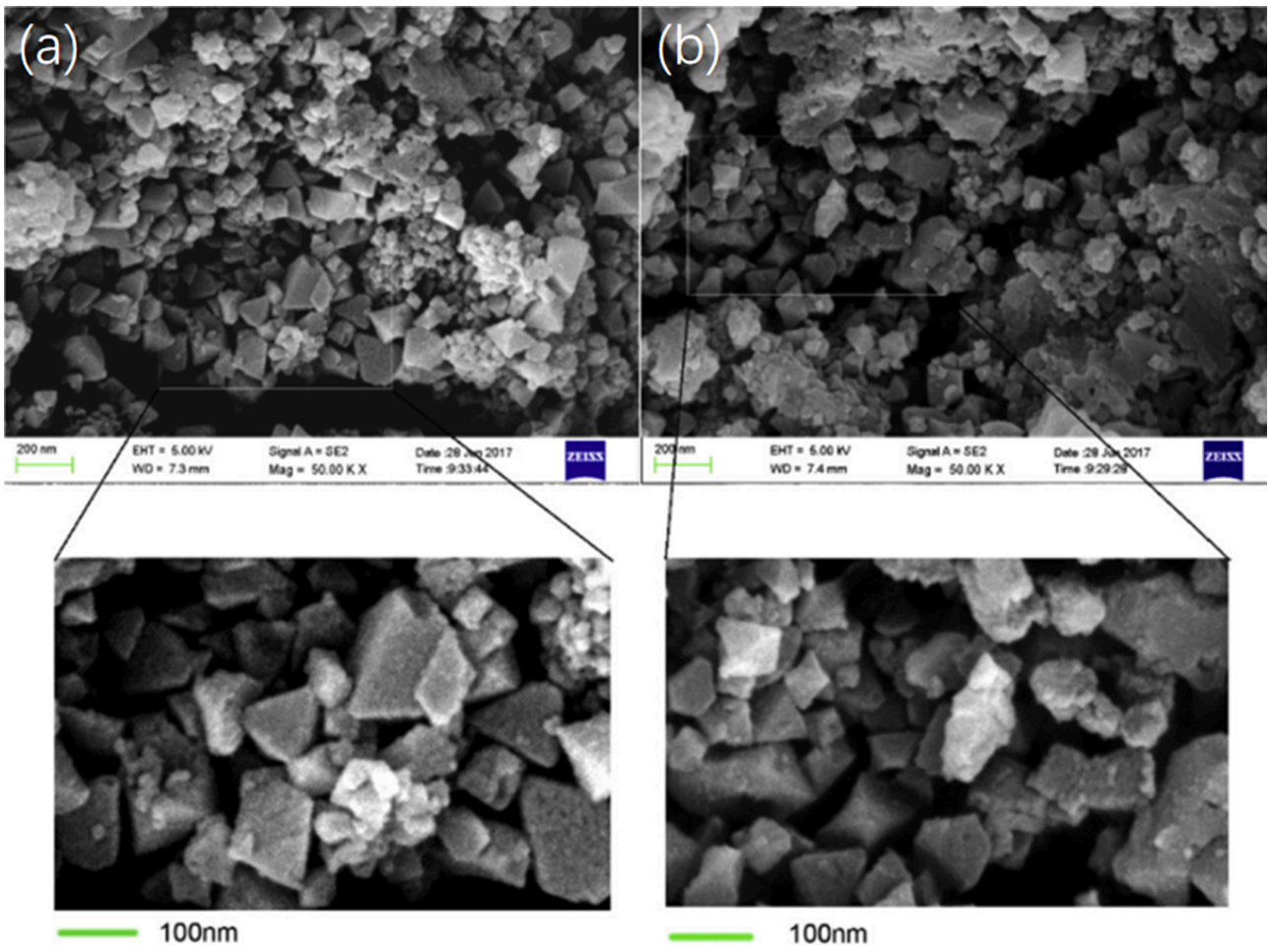

Fig. 17. SEM images of (a) MIL-100(Fe) and (b) Fe_2O_3–2S [178].

MnFeCo layered double hydroxide (LDO) catalyst had a NO conversion rate of more than 86% between 50 and 400 °C [179]. As shown in Fig. 18 (a), the ternary MnFeCo-LDH nanosheet has a regular shape, distribution, and order, small size distribution, and retains typical LDH crystal structure and morphology. It can be confirmed that Mn and Fe-Co occupy and retain M^{2+} and M^{3+} cationic crystal positions, respectively. In addition, Fig. 18(c-f) shows that the MnFeCo-LDO obtained by calcination has a uniform distribution of Mn, Fe, Co and O elements. Together, these contribute to the synergistic interaction between Mn, Fe and Co species, forming amorphous metal oxides, and releasing oxygen

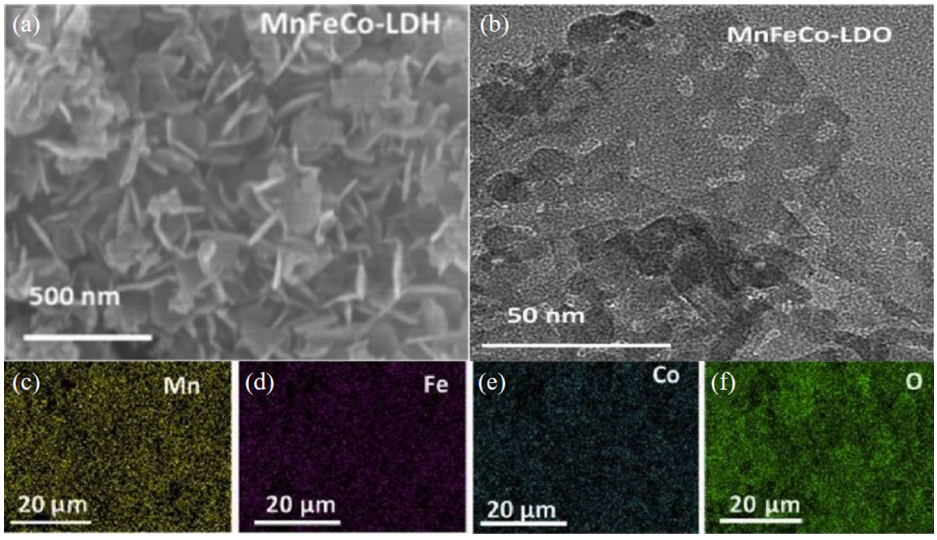

Fig. 18. (a) SEM image of MnFeCo-LDH sample; TEM characterization images of (b) MnFeCo-LDO samples. The corresponding EDX mapping analysis of the MnFeCo-LDO sample showing (c) Mn, (d) Fe, (e) Co, and (f) O element distribution maps [179].

more easily at low temperatures, enhancing the reduction power of the catalyst.

In conclusion, we found that the catalytic performance of the catalysts can be improved by changing the morphology. The porous and macro-porous structure can provide more mass transfer channels for the reaction gas, thereby effectively promoting the contact between the reaction gas and the catalyst surface, resulting in better activation and adsorption. The morphology similar to the core-shell structure can effectively prevent the binding of toxic gasses to the active sites of the catalyst and prevent the deactivation of the catalyst. However, how to produce this morphology on a commercial scale is also a difficult problem, and how to maintain the stability of the morphology of catalysts in practical applications with porous, macroporous, and core-shell structures is also an important problem in the long-term use of catalysts.

5. Conclusions and outlook

Based on the above studies, Fe-based catalysts have been shown to have high SCR activity and SO_2 resistance, which have obvious advantages for removing NO_x from industrial flue gas and automobile exhaust. Although the SCR activity of a single FeO_x catalyst is not high, the redox characteristics, surface acidity, and catalytic performance of Fe-based catalysts are effectively regulated by the synergistic effects among elements. In this paper, the synergy between different elements and Fe, and the effects of some unique morphology on the SCR activity of Fe-based catalysts are reviewed. The improvement of the physicochemical properties of the catalyst by the synergy between the elements is emphasized, and the electron transfer between the elements is promoted by designing different preparation processes. In addition, the excellent SCR activity of Fe-based catalysts provides a new idea for the development of Fe-based catalysts with more practical value in the future. However, the rapid progress of Fe-based catalysts in the laboratory cannot be used directly as commercial catalysts, and the following issues still need to be addressed.

(1) In the practical application of the catalyst, along with pollutants such as SO_2, H_2O, alkali metals, heavy metals, and soot will be adsorbed on the surface of the catalyst, resulting in poisoning and deactivation of the active sites on the surface of the catalyst. Therefore, the resistance of Fe-based catalysts to various pollutants must meet basic indicators. In addition, the poisoning mechanism of the Fe-based catalyst surface also needs to be further analyzed.
(2) During the operation of the diesel engine, the exhaust temperature of the exhaust gas may exceed 950 °C. If the Fe-based catalyst does not have sufficient thermal stability at this temperature, it will lead to the collapse of the catalyst structure and cause sintering, which will affect the service life and catalytic activity of the catalyst. In addition, severe vibrations during driving and the impact of exhaust gas flow in the exhaust may cause the catalyst to shatter. Therefore, the catalyst also needs to have strong mechanical strength and thermal stability.
(3) For a long time, scholars have done extensive research on the synergistic effects between different elements, and it is believed that the synergistic effects between elements can have a huge impact on the SCR activity of Fe-based catalysts. To better develop SCR catalysts, we should further analyze the root causes of the electron transport ability and adsorption ability generated by the synergistic effects.
(4) On account of the insufficient low-temperature activity of Fe-based catalysts themselves, most of the studies so far have been based on element doping to improve the low-temperature activity of Fe-based catalysts. It was found that the catalyst's SCR activity was improved due to the synergistic effects between elements after doping. Then a simple physical and chemical analysis was carried out, and it was found that the catalyst's redox performance, surface acidity, BET surface area, and dispersion were improved, but the root cause of the increase in the catalyst's SCR activity was not further analyzed.
(5) In laboratory studies, catalysts are often simply tested for performance within a few hours. However, when working under real conditions, the catalyst is often used for a long time, and the long-term application may lead to the phenomenon of deactivation due to the insufficient durability of the catalyst. Therefore, the catalyst should have sufficient durability and stability.

Declaration of Competing Interest

The authors declare that they have no known competing financial interests or personal relationships that could have appeared to influence the work reported in this paper.

Data availability

Data will be made available on request.

Acknowledgments

This work was supported by the Scientific and Technological Innovation Team Project of the Shaanxi Innovation Capability Support Plan, China (2022TD-30), the Youth Innovation Team of Shaanxi Universities (2019–2022), the top young talents project of "Special support program for high-level talents" in the Shaanxi Province (2018–2023), and the International Science and Technology Cooperation Program of the Shaanxi Province (2022KW-39).

References

[1] G.C. Dhal, S. Dey, D. Mohan, R. Prasad, Study of Fe, Co, and Mn-based perovskite-type catalysts for the simultaneous control of soot and NOx from diesel engine exhaust, Mater. Discov. 10 (2017) 37–42.
[2] B. Roy, W.L. Choo, S. Bhattacharya, Prediction of distribution of trace elements under Oxy-fuel combustion condition using Victorian brown coals, Fuel 114 (2013) 135–142.
[3] H.S. John, Urban air pollution: state of the science, Science 243 (1989) 745–752.
[4] Z. Liu, J. Hao, L. Fu, T. Zhu, Study of Ag/La0.6Ce0.4CoO3 catalysts for direct decomposition and reduction of nitrogen oxides with propene in the presence of oxygen, Appl. Catal. B 44 (2003) 355–370.
[5] A. Halepoto, M. Kashif, Y. Su, J. Cheng, W. Deng, B. Zhao, Preparations and characterization on Fe based catalyst supported on coconut shell activated carbon CS(AC) and SCR of NOx-HC, Catal. Surv. Asia 24 (2020) 123–133.
[6] Y. Zhang, H. Zeng, B. Jia, Z. Liu, Selective catalytic reduction of NOx by H-2 over a novel Pd/FeTi catalyst, Catal. Today 360 (2021) 213–219.
[7] J.K. Lai, N.R. Jaegers, B.M. Lis, M. Guo, M.E. Ford, E. Walter, Y. Wang, J.Z. Hu, I. E. Wachs, Structure-activity relationships of hydrothermally aged titania-supported vanadium-tungsten oxide catalysts for SCR of NOx emissions with NH3, ACS Catal. 11 (2021) 12096–12111.
[8] N.Y. Topsoe, Mechanism of the selective catalytic reduction of nitric oxide by ammonia elucidated by in situ on-line fourier transform infrared spectroscopy, Science 265 (1994) 1217–1219.
[9] F. Gao, D. Mei, Y. Wang, J. Szanyi, C.H.F. Peden, Selective catalytic reduction over Cu/SSZ-13: linking homo- and heterogeneous catalysis, J. Am. Chem. Soc. 139 (2017) 4935–4942.
[10] W. Shan, F. Liu, H. He, X. Shi, C. Zhang, A superior Ce-W-Ti mixed oxide catalyst for the selective catalytic reduction of NOx with NH3, Appl. Catal. B 115-116 (2012) 100–106.
[11] B. Jiang, B. Deng, Z. Zhang, Z. Wu, X. Tang, S. Yao, H. Lu, Effect of Zr addition on the low-temperature SCR activity and SO2 tolerance of Fe-Mn/Ti catalysts, J. Phys. Chem. C 118 (2014) 14866–14875.
[12] L. Chen, J. Li, M. Ge, Promotional effect of Ce-doped V2O5-WO3/TiO2 with low vanadium loadings for selective catalytic reduction of NOx by NH3, J. Phys. Chem. C 113 (2009) 21177–21184.
[13] M. Casanova, K. Schermanz, J. Llorca, A. Trovarelli, Improved high temperature stability of NH3-SCR catalysts based on rare earth vanadates supported on TiO2-WO3-SiO2, Catal. Today 184 (2012) 227–236.
[14] L. Chen, J. Li, M. Ge, DRIFT study on cerium-tungsten/titania catalyst for selective catalytic reduction of NOx with NH3, Environ. Sci. Technol. 44 (2010) 9590–9596.
[15] R.Q. Long, R.T. Yang, Superior Fe-ZSM-5 catalyst for selective catalytic reduction of nitric oxide by ammonia, J. Am. Chem. Soc. 121 (1999) 5595–5596.

[16] Z. Lian, F. Liu, H. He, Enhanced activity of Ti-modified V2O5/CeO2 catalyst for the selective catalytic reduction of NOx with NH3, Ind. Eng. Chem. Res. 53 (2014) 19506–19511.
[17] G. Busca, L. Lietti, G. Ramis, F. Berti, Chemical and mechanistic aspects of the selective catalytic reduction of NOx by ammonia over oxide catalysts: a review, Appl. Catal. B 18 (1998) 1–36.
[18] G. Qi, R.T. Yang, R. Chang, MnOx-CeO2 mixed oxides prepared by co-precipitation for selective catalytic reduction of NO with NH3 at low temperatures, Appl. Catal. B 51 (2004) 93–106.
[19] B. Shen, T. Liu, N. Zhao, X. Yang, L. Deng, Iron-doped Mn-Ce/TiO2 catalyst for low temperature selective catalytic reduction of NO with NH3, J. Environ. Sci. 22 (2010) 1447–1454.
[20] X. Wang, K. Gui, Fe2O3 particles as superior catalysts for low temperature selective catalytic reduction of NO with NH3, J. Environ. Sci. 25 (2013) 2469–2475.
[21] S. Yang, C. Liu, H. Chang, L. Ma, Z. Qu, N. Yan, C. Wang, J. Li, Improvement of the activity of gamma-Fe2O3 for the selective catalytic reduction of NO with NH3 at high temperatures: NO reduction versus NH3 oxidization, Ind. Eng. Chem. Res. 52 (2013) 5601–5610.
[22] F. Li, Z. Sun, S. Luo, L.S. Fan, Ionic diffusion in the oxidation of iron-effect of support and its implications to chemical looping applications, Energy Environ. Sci. 4 (2011) 876–880.
[23] T.J. Huang, Y.P. Zhang, K. Zhuang, B. Lu, Y.W. Zhu, K. Shen, Preparation of honeycombed holmium-modified Fe-Mn/TiO2 catalyst and its performance in the low temperature selective catalytic reduction of NOx, J. Fuel Chem. Technol. 46 (2018) 319–327.
[24] E. Hums, Is advanced SCR technology at a standstill? A provocation for the academic community and catalyst manufacturers, Catal. Today 42 (1998) 25–35.
[25] G. Busca, L. Lietti, G. Ramis, Francesco, Chemical and mechanistic aspects of the selective catalytic reduction of NOx by ammonia over oxide catalysts: a review, Appl. Catal. B 18 (1998) 1–36.
[26] S. Ma, H. Tan, Y. Li, P. Wang, C. Zhao, X. Niu, Y. Zhu, Excellent low-temperature NH3-SCR NO removal performance and enhanced H2O resistance by Ce addition over the Cu0.02Fe0.2CeyTi1-yOx (y = 0.1, 0.2, 0.3) catalysts, Chemosphere 243 (2020), 125309.
[27] J. Yu, F. Guo, Y. Wang, J. Zhu, Y. Liu, F. Su, S. Gao, G. Xu, Sulfur poisoning resistant mesoporous Mn-base catalyst for low-temperature SCR of NO with NH3, Appl. Catal. B 95 (2010) 160–168.
[28] H. Chen, W. Ning, C. Chen, T. Zhang, Influence of Fe2O3 crystal phase on the performance of Fe-based catalysts for CO2 hydrogenation, J. Fuel Chem. Technol. 43 (2015) 1387–1392.
[29] H. Wang, P. Ning, Y. Zhang, Y. Ma, J. Wang, L. Wang, Q. Zhang, Highly efficient WO3-FeOx catalysts synthesized using a novel solvent-free method for NH3-SCR, J. Hazard. Mater. 388 (2020), 121812.
[30] Y. Geng, S. Xiong, B. Li, Y. Peng, S. Yang, Promotion of H3PW12O40 grafting on NOx abatement over γ-Fe2O3: performance and reaction mechanism, Ind. Eng. Chem. Res. 57 (2018) 13661–13670.
[31] Y. Zeng, W. Song, Y. Wang, S. Zhang, T. Wang, Q. Zhong, Novel Fe-doped CePO4 catalyst for selective catalytic reduction of NO with NH3: the role of Fe3+ ions, J. Hazard. Mater. 383 (2020), 121212.
[32] G. Ferey, C. Serre, C. Mellot-Draznieks, F. Millange, S. Surble, J. Dutour, I. Margiolaki, A hybrid solid with giant pores prepared by a combination of targeted chemistry, simulation, and powder diffraction, Angew. Chem. Int. Ed. Engl. 43 (2004) 6296–6301.
[33] G. Qi, R.T. Yang, Characterization and FTIR studies of MnO x CeO 2 catalyst for low-temperature selective catalytic reduction of NO with NH 3, Appl. Catal. B 108 (2004) 15738–15747.
[34] S. Yang, C. Wang, J. Chen, Y. Peng, L. Ma, H. Chang, L. Chen, C. Liu, J. Xu, J.-. Li, A novel magnetic Fe-Ti-V spinel catalyst for the selective catalytic reduction of NO with NH3 in a broad temperature range, Catal. Sci. Technol. 2 (2012) 915–917.
[35] F. Liu, H. He, Y. Ding, C. Zhang, Effect of manganese substitution on the structure and activity of iron titanate catalyst for the selective catalytic reduction of NO with NH3, Appl. Catal. B 93 (2009) 3760–3769.
[36] S. Ma, X. Zhao, Y. Li, T. Zhang, F. Yuan, X. Niu, Y. Zhu, Effect of W on the acidity and redox performance of the Cu0.02Fe0.2WaTiOx (a = 0.01, 0.02, 0.03) catalysts for NH3-SCR of NO, Appl. Catal. B 248 (2019) 226–238.
[37] X. Li, J. Chen, C. Lu, G. Luo, H. Yao, Performance of Mo modified γ-Fe2O3 catalyst for selective catalytic reduction of NOx with ammonia: presence of arsenic in flue gas, Fuel 294 (2021), 120552.
[38] Z. Wu, B. Jiang, Y. Liu, H. Wang, R. Jin, DRIFT study of manganese/titania-based catalysts for low-temperature selective catalytic reduction of NO with NH3, Environ. Sci. Technol. 41 (2007) 5812–5817.
[39] Z. Fan, J.W. Shi, C. Gao, G. Gao, B. Wang, C. Niu, Rationally designed porous MnOx-FeOx nanoneedles for low-temperature selective catalytic reduction of NOx by NH3, ACS Appl. Mater. Interfaces 9 (2017) 16117–16127.
[40] L. Liu, S. Su, D. Chen, T. Shu, X. Zheng, J. Yu, Y. Feng, Y. Wang, S. Hu, J. Xiang, Highly efficient NH3-SCR of NOx over MnFeW/Ti catalyst at low temperature: SO2 tolerance and reaction mechanism, Fuel 307 (2022), 121805.
[41] J. Zhang, Z. Huang, Y. Du, F. Sanchez-Ochoa, X. Wu, G. Jing, Identification of active sites over Fe2O3-based architecture: the promotion effect of H2SO4 erosion synthetic protocol, ACS Appl. Energy Mater. 1 (2018) 2385–2391.
[42] Z. Fu, G. Zhang, W. Han, Z. Tang, The water resistance enhanced strategy of Mn based SCR catalyst by construction of TiO2 shell and superhydrophobic coating, Chem. Eng. J. 426 (2021), 131334.
[43] Y. Zhu, X. Xiao, J. Wang, C. Ma, X. Jia, W. Qiao, L. Ling, Enhanced activity and water resistance of hierarchical flower-like Mn-Co binary oxides for ammonia-SCR reaction at low temperature, Appl. Surf. Sci. 569 (2021), 150989.
[44] A. Fan, Y. Jing, J. Guo, X. Shi, S. Yuan, J. Li, Investigation of Mn doped perovskite La-Mn oxides for NH3-SCR activity and SO2/H2O resistance, Fuel 310 (2022), 122237.
[45] X. Tang, C. Wang, F. Gao, Y. Ma, H. Yi, S. Zhao, Y. Zhou, Effect of hierarchical element doping on the low-temperature activity of manganese-based catalysts for NH3-SCR, J. Environ. Chem. Eng. 8 (2020), 104399.
[46] J. Tan, Y. Wei, Y. Sun, J. Liu, Z. Zhao, W. Song, J. Li, X. Zhang, Simultaneous removal of NOx and soot particulates from diesel engine exhaust by 3DOM Fe-Mn oxide catalysts, J. Ind. Eng. Chem. 63 (2018) 84–94.
[47] Y. Wei, K. Gui, X. Liu, H. Liang, S. Gu, D. Ren, Performance of Mn-Ce co-doped siderite catalysts in the selective catalytic reduction of NOx by NH3, J. Fuel Chem. Technol. 47 (2019) 1495–1503.
[48] C. Zhang, T. Chen, H. Liu, D. Chen, B. Xu, C. Qing, Low temperature SCR reaction over Nano-Structured Fe-Mn Oxides: characterization, performance, and kinetic study, Appl. Surf. Sci. 457 (2018) 1116–1125.
[49] L. Lin, C. Lee, Y. Zhang, H. Bai, Aerosol-assisted deposition of Mn-Fe oxide catalyst on TiO2 for superior selective catalytic reduction of NO with NH3 at low temperatures, Catal. Commun. 111 (2018) 36–41.
[50] S. Zhang, Y. Zhao, J. Yang, J. Zhang, C. Zheng, Fe-modified MnOx/TiO2 as the SCR catalyst for simultaneous removal of NO and mercury from coal combustion flue gas, Chem. Eng. J. 348 (2018) 618–629.
[51] X. Wang, S. Wu, W. Zou, S. Yu, K. Gui, L. Dong, Fe-Mn/Al2O3 catalysts for low temperature selective catalytic reduction of NO with NH3, Chin. J. Catal. 37 (2016) 1314–1323.
[52] S. Chen, Q. Yan, C. Zhang, Q. Wang, A novel highly active and sulfur resistant catalyst from Mn-Fe-Al layered double hydroxide for low temperature NH3-SCR, Catal. Today 327 (2019) 81–89.
[53] D. Ren, K. Gui, S. Gu, Y. Wei, Mechanism of improving the SCR NO removal activity of Fe2O3 catalyst by doping Mn, J. Alloys Compd. 867 (2021), 158787.
[54] J. Chen, L. Guo, H. Zhu, Y. Qiu, D. Yin, T. Zhang, J. Chen, Y. Peng, J. Li, Balancing redox and acidic properties for optimizing catalytic performance of SCR catalysts: a case study of nanopolyhedron CeOx-supported WOx, J. Environ. Chem. Eng. 9 (2021), 105828.
[55] G.J. Kim, S.H. Lee, K.B. Nam, S.C. Hong, A study on the structure of tungsten by the addition of ceria: effect of monomeric structure over W/Ce/TiO2 catalyst on the SCR reaction, Appl. Surf. Sci. 507 (2020), 145064.
[56] Z. Liu, H. Su, B. Chen, J. Li, S.I. Woo, Activity enhancement of WO3 modified Fe2O3 catalyst for the selective catalytic reduction of NOx by NH3, Chem. Eng. J. 299 (2016) 255–262.
[57] F. Liu, W. Shan, Z. Lian, J. Liu, H. He, The smart surface modification of Fe2O3 by WOx for significantly promoting the selective catalytic reduction of NOx with NH3, Appl. Catal. B 230 (2018) 165–176.
[58] J. Zhang, Z. Huang, Y. Du, X. Wu, H. Shen, G. Jing, Atomic-scale insights into the nature of active sites in Fe2O3-supported submonolayer WO3 catalysts for selective catalytic reduction of NO with NH3, Chem. Eng. J. 381 (2020), 122668.
[59] C. Li, Z. Xiong, J. He, X. Qu, Z. Li, X. Ning, W. Lu, S. Wu, L. Tan, Influence of ignition atmosphere on the structural properties of magnetic iron oxides synthesized via solution combustion and the NH3-SCR activity of W/Fe2O3 catalyst, Appl. Catal. A Gen. 602 (2020), 117726.
[60] Q. Zhang, Y. Zhang, T. Zhang, H. Wang, Y. Ma, J. Wang, P. Ning, Influence of preparation methods on iron-tungsten composite catalyst for NH3-SCR of NO: the active sites and reaction mechanism, Appl. Surf. Sci. 503 (2020), 144190.
[61] T. Zhang, Y. Zhang, P. Ning, H. Wang, Y. Ma, S. Xu, M. Liu, Q. Zhang, F. Xia, The property tuning of NH3-SCR over iron-tungsten catalyst: role of calcination temperature on surface defect and acidity, Appl. Surf. Sci. 538 (2021), 147999.
[62] X. Liu, P. Ning, H. Li, Z.X. Song, Y.C. Wang, J.H. Zhang, X.S. Tang, M.Z. Wang, Q. L. Zhang, Probing NH3-SCR catalytic activity and SO2 resistance over aqueous-phase synthesized Ce-W@TiO2 catalyst, J. Fuel Chem. Technol. 44 (2016) 225–231.
[63] X. Wang, R. Duan, W. Liu, D. Wang, B. Wang, Y. Xu, C. Niu, J.W. Shi, The insight into the role of CeO2 in improving low-temperature catalytic performance and SO2 tolerance of MnCoCeOx microflowers for the NH3-SCR of NOx, Appl. Surf. Sci. 510 (2020), 145517.
[64] C. Chen, H. Xie, P. He, X. Liu, C. Yang, N. Wang, C. Ge, Comparison of low-temperature catalytic activity and H2O/SO2 resistance of the Ce-Mn/TiO2 NH3-SCR catalysts prepared by the reverse co-precipitation, co-precipitation and impregnation method, Appl. Surf. Sci. 571 (2022), 151285.
[65] K. Zhao, W. Han, G. Lu, J. Lu, Z. Tang, X. Zhen, Promotion of redox and stability features of doped Ce–W–Ti for NH3-SCR reaction over a wide temperature range, Appl. Surf. Sci. 379 (2016) 316–322.
[66] L. Zhu, J. Yao, G. Ma, P. Cao, S. Wu, Z. Li, NH3-SCR performance and SO2 resistance comparison of CeO2 based catalysts with Fe/Mo additive surface decoration, Chem. Eng. J. 428 (2022), 131372.
[67] K. Zhang, J. Wang, P. Guan, N. Li, Z. Gong, R. Zhao, H. Luo, W. Wu, Low-temperature NH3-SCR catalytic characteristic of Ce-Fe solid solutions based on rare earth concentrate, Mater. Res. Bull. 128 (2020), 110871.
[68] H. Chitsazi, N. Zhang, L. Li, X. Liu, R. Wu, J. He, L. Song, H. He, In-situ DRIFT assessment on strengthening effect of cerium over FeOx/TiO2 catalyst for selective catalytic reduction of NOx with NH3, J. Rare Earths 39 (2021) 526–531.
[69] X. Wang, L. Zhang, S. Wu, W. Zou, S. Yu, Y. Shao, L. Dong, Promotional effect of Ce on iron-based catalysts for selective catalytic reduction of NO with NH3, Catalysts 6 (2016) 112.

[70] Y. Shu, T. Aikebaier, X. Quan, S. Chen, H. Yu, Selective catalytic reaction of NOx with NH3 over Ce-Fe/TiO2-loaded wire-mesh honeycomb: resistance to SO2 poisoning, Appl. Catal. B Environ. 150 (2014) 630–635.
[71] Z. Zhou, W. Li, Z. Liu, Significantly Enhanced Catalytic Performance of Fe-2(SO4)(3)/CeO2 Catalyst for the Selective Catalytic Reduction of NOx by NH3, Ind. Eng. Chem. Res. 60 (2021) 15472–15478.
[72] X. Zhang, J. Wang, Z. Song, H. Zhao, Y. Xing, M. Zhao, J. Zhao, Z.A. Ma, P. Zhang, N. Tsubaki, Promotion of surface acidity and surface species of doped Fe and SO42- over CeO2 catalytic for NH3-SCR reaction, Mol. Catal. 463 (2019) 1–7.
[73] X. Zhang, T. Zhang, Z. Song, W. Liu, Y. Xing, Effect of sulfate species on the performance of Ce-Fe-Ox catalysts in the selective catalytic reduction of NO by NH3, J. Fuel Chem. Technol. 49 (2021) 844–852.
[74] D. Ren, K. Gui, S. Gu, Comparison of sulfur poisoning resistance of Ce/Mn doped gamma-Fe2O3 (001) surface in NH3-SCR reaction with DFT method, Appl. Surf. Sci. 561 (2021), 149847.
[75] S.B. Rasmussen, B.L. Abrams, Fundamental chemistry of V-SCR catalysts at elevated temperatures, Catal. Today 297 (2017) 60–63.
[76] M. Olga Guerrero-Perez, Supported, bulk and bulk-supported vanadium oxide catalysts: a short review with an historical perspective, Catal. Today 285 (2017) 226–233.
[77] D.W. Kwon, K.H. Park, S.C. Hong, Enhancement of SCR activity and SO2 resistance on VOx/TiO2 catalyst by addition of molybdenum, Chem. Eng. J. 284 (2016) 315–324.
[78] D.W. Kwon, S. Lee, J. Kim, K.Y. Lee, H.P. Ha, Influence of support composition on enhancing the performance of Ce-V on TiO2 comprised tungsten-silica for NH3-SCR, Catal. Today 359 (2021) 112–123.
[79] Y. Xing, H. Zhang, W. Su, K. Li, J. Zhang, J. Shi, J. Tian, J. Wang, Mineral-derived catalysts optimized for selective catalytic reduction of NOx with NH3, J. Clean. Prod. 289 (2021), 125756.
[80] J. Mu, X. Li, W. Sun, S. Fan, X. Wang, L. Wang, M. Qin, G. Gan, Z. Yin, D. Zhang, Inductive effect boosting catalytic performance of advanced Fe1-xVxO delta catalysts in low-temperature NH3 selective catalytic reduction: insight into the structure, interaction, and mechanisms, ACS Catal. 8 (2018) 6760–6774.
[81] H. Huang, Y. Chen, R. Yang, Q. Zhu, H. Lu, Fe-V/TiO2 catalysts for selective catalytic reduction of NOx with NH3 in diesel exhaust, J. Fuel Chem. Technol. 42 (2014) 751–757.
[82] N. Zhu, W. Shan, Z. Lian, Y. Zhang, K. Liu, H. He, A superior Fe-V-Ti catalyst with high activity and SO2 resistance for the selective catalytic reduction of NOx with NH3, J. Hazard. Mater. 382 (2020), 120970.
[83] J. Liu, X. Yang, C. Zhang, F. Wu, Z. Li, Q. Xia, Effect of Fe2O3 on surface properties and activities of V2O5-WO3/TiO2 catalysts, CIESC J. 67 (2016) 1287–1293.
[84] T.H. Kang, S. Youn, D.H. Kim, Improved catalytic performance and resistance to SO2 over V2O5-WO3/TiO2 catalyst physically mixed with Fe2O3 for low-temperature NH3-SCR, Catal. Today 376 (2021) 95–103.
[85] M.H. Kim, K.H. Yang, The role of Fe2O3 species in depressing the formation of N2O in the selective reduction of NO by NH3 over V2O5/TiO2-based catalysts, Catalysts 8 (2018) 134.
[86] N.T.P. Thao, K.H. Yang, M.H. Kim, Y.S. Hong, Selective catalytic reduction of NO by NH3 over Fe2O3-promoted V2O5/TiO2-based catalysts with high Fe2O3-to-V2O5 ratios, Catal. Today 360 (2021) 305–316.
[87] S. Liu, H. Wang, Y. Wei, R. Zhang, Core-shell structure effect on CeO2 and TiO2 supported WO3 for the NH3-SCR process, Mol. Catal. 485 (2020), 110822.
[88] X. Wang, Z. Zhao, Y. Xu, Q. Li, Promoting effect of Ti addition on three-dimensionally ordered macroporous Mn-Ce catalysts for NH3-SCR reaction: enhanced N-2 selectivity and remarkable water resistance, Appl. Surf. Sci. 569 (2021), 151047.
[89] C. Liu, Y. Bi, H. Wang, Z. Zhang, J. Wang, M. Guo, Q. Liu, Promotional effects on NH3-SCR performance of CeO2-SnO2 catalysts doped by TiO2: a mechanism study, Catal. Surv. Asia 25 (2021) 48–57.
[90] Y. Geng, X. Chen, S. Yang, F. Liu, W. Shan, Promotional effects of Ti on a CeO2-MoO3 catalyst for the selective catalytic reduction of NOx with NH3, ACS Appl. Mater. Interfaces 9 (2017) 16952–16959.
[91] Y. Zhou, Z. Xie, J. Jiang, J. Wang, X. Song, Q. He, W. Ding, Z. Wei, Lattice-confined Ru clusters with high CO tolerance and activity for the hydrogen oxidation reaction (vol 3, pg 454, 2020), Nat. Catal. 4 (2021), 341-341.
[92] D. Wang, J. Wu, S. Niu, C. Lu, L. Xu, H. Yu, J. Li, Structural property of gamma-Fe2O3 catalysts doped with Sn and Ti and their activity in the selective catalytic reduction of NOx, J. Fuel Chem. Technol. 43 (2015) 876–883.
[93] J. Sun, Y. Lu, L. Zhang, C. Ge, C. Tang, H. Wan, L. Dong, Comparative study of different doped metal cations on the reduction, acidity, and activity of Fe9M1Ox (M = Ti4+, Ce4+/3+, Al3+) catalysts for NH3-SCR reaction, Ind. Eng. Chem. Res. 56 (2017) 12101–12110.
[94] T. Boningari, D.K. Pappas, P.G. Smirniotis, Metal oxide-confined interweaved titania nanotubes M/TNT (M = Mn, Cu, Ce, Fe, V, Cr, and Co) for the selective catalytic reduction of NOx in the presence of excess oxygen, J. Catal. 365 (2018) 320–333.
[95] Y. Li, Z. Liu, X. Li, Y. Hou, Research on structure-activity relationship dominated by template agents for mesoporous FeTi catalysts in SCR of NO with NH3, Mol. Catal. 509 (2021), 111635.
[96] K. Guo, J. Ji, R. Osuga, Y. Zhu, J. Sun, C. Tang, J.N. Kondo, L. Dong, Construction of Fe2O3 loaded and mesopore confined thin-layer titania catalyst for efficient NH3-SCR of NOx with enhanced H2O/SO2 tolerance, Appl. Catal. B Environ. 287 (2021), 119982.
[97] L. Song, K. Ma, W. Tian, J. Ji, C. Liu, S. Tang, W. Jiang, H. Yue, B. Liang, An environmentally friendly FeTiSOx catalyst with a broad operation-temperature window for the NH3-SCR of NOx, AlChE J. 65 (2019) e16684.
[98] D. Xu, W. Wu, P. Wang, J. Deng, T. Yan, D. Zhang, Boosting the alkali/heavy metal poisoning resistance for no removal by using iron-titanium pillared montmorillonite catalysts, J. Hazard. Mater. 399 (2020), 122947.
[99] Y. Wei, H. Fan, R. Wang, Transition metals (Co, Zr, Ti) modified iron-samarium oxide as efficient catalysts for selective catalytic reduction of NOx at low-temperature, Appl. Surf. Sci. 459 (2018) 63–73.
[100] L. Xu, S. Niu, D. Wang, C. Lu, Q. Zhang, K. Zhang, J. Li, Selective catalytic reduction of NOx with NH3 over titanium modified FexMgyOz catalysts: performance and characterization, J. Ind. Eng. Chem. 63 (2018) 391–404.
[101] J. Chen, W. Qu, Y. Chen, X. Liu, X. Jiang, H. Wang, Y. Zong, Z. Ma, X. Tang, Simultaneously enhancing stability and activity of maghemite via site-specific Ti (IV) doping for NO emission control, ChemCatChem 10 (2018) 4683–4688.
[102] Y. Tan, F. Li, B. Zhao, W. Chen, M. Tian, Hydrothermal synthesis of a Ce-Zr-Ti mixed oxide catalyst with enhanced catalytic performance for a NH3-SCR reaction, Langmuir 37 (2021) 14823–14832.
[103] I. Salem, X. Courtois, E.C. Corbos, P. Marecot, D. Duprez, NO conversion in presence of O2, H2O and SO2: improvement of a Pt/Al2O3 catalyst by Zr and Sn, and influence of the reducer C3H6 or C3H8, Catal. Commun. 9 (2008) 664–669.
[104] X. Wei, R. Zhao, B. Chu, S. Xie, Q. qin, K. Chen, L. Li, S. Zhao, B. Li, L. Dong, Significantly enhanced activity and SO2 resistance of Zr-modified CeTiOx catalyst for low-temperature NH3-SCR by H2 reduction treatment, Mol. Catal. 518 (2022), 112069.
[105] Z. Chen, Q. Liu, L. Guo, S. Zhang, L. Pang, Y. Guo, T. Li, The promoting mechanism of in situ Zr doping on the hydrothermal stability of Fe-SSZ-13 catalyst for NH3-SCR reaction, Appl. Catal. B 286 (2021), 119816.
[106] B. Jia, J. Guo, S. Shu, N. Fang, J. Li, Y. Chu, Effects of different Zr/Ti ratios on NH3–SCR over MnOx/ZryTi1-yO2: characterization and reaction mechanism, Mol. Catal. 443 (2017) 25–37.
[107] B. Fan, Z. Zhang, C. Liu, Q. Liu, Investigation of sulfated iron-based catalysts with different sulfate position for selective catalytic reduction of NOx with NH3, Catalysts 10 (2020) 1035.
[108] C. Liu, H. Wang, Y. Bi, Z. Zhang, A study on the selective catalytic reduction of NOx by ammonia on sulphated iron-based catalysts, RSC Adv. 10 (2020) 40948–40959.
[109] K. Kang, X. Yao, Y. Huang, J. Cao, J. Rong, W. Zhao, W. Luo, Y. Chen, Insights into the co-doping effect of Fe3+ and Zr4+ on the anti-K performance of CeTiOx catalyst for NH3-SCR reaction, J. Hazard. Mater. 416 (2021), 125821.
[110] C. Liu, Y. Bi, J. Li, Activity enhancement of sulphated Fe2O3 supported on TiO2–ZrO2 for the selective catalytic reduction of NO by NH3, Appl. Surf. Sci. 528 (2020), 146695.
[111] R. Foo, T. Vazhnova, D.B. Lukyanov, P. Millington, J. Collier, R. Rajaram, S. Golunski, Formation of reactive Lewis acid sites on Fe/WO3-ZrO2 catalysts for higher temperature SCR applications, Appl. Catal. B Environ. 162 (2015) 174–179.
[112] K. Swirk, Y. Wang, C. Hu, L. Li, P. Da Costa, G. Delahay, Novel preparation of Cu and Fe zirconia supported catalysts for selective catalytic reduction of NO with NH3, Catalysts 11 (2021) 55.
[113] Z. Han, Q. Yu, H. Xie, K. Liu, Q. Qin, Z. Xue, Fabrication of manganese-based Zr-Fe polymeric pillared interlayered montmorillonite for low-temperature selective catalytic reduction of NOx by NH3 in the metallurgical sintering flue gas, Environ. Sci. Pollut. Res. 25 (2018) 32122–32129.
[114] Z. Han, Q. Yu, Z. Xue, K. Liu, Q. Qin, Sm-doped manganese-based Zr-Fe polymeric pillared interlayered montmorillonite for low temperature selective catalytic reduction of NOx by NH3 in metallurgical sintering flue gas, RSC Adv. 8 (2018) 42017–42024.
[115] Y. Zhu, Y. Zhang, R. Xiao, T. Huang, K. Shen, Novel holmium-modified Fe-Mn/TiO2 catalysts with a broad temperature window and high sulfur dioxide tolerance for low-temperature SCR, Catal. Commun. 88 (2017) 64–67.
[116] L. Xu, S. Niu, C. Lu, D. Wang, K. Zhang, J. Li, NH3-SCR performance and characterization over magnetic iron-magnesium mixed oxide catalysts, Korean J. Chem. Eng. 34 (2017) 1576–1583.
[117] C. Shao, X. Liu, D. Meng, Q. Xu, Y. Guo, Y. Guo, W. Zhan, L. Wang, G. Lu, Catalytic performance of Co-Fe mixed oxide for NH3-SCR reaction and the promotional role of cobalt, RSC Adv. 6 (2016) 66169–66179.
[118] J. Chen, B. Zhu, T. Du, Y. Sun, Z. Zhu, S. Yin, D. Zhang, Low-temperature selective catalytic reduction of NOx with NH3 over Co modified Fe2O3/AC catalysts, Nonferrous Met. Eng. 7 (2017) 99–102.
[119] B. Shen, S. Zhu, X. Zhang, G. Chi, D. Patel, M. Si, C. Wu, Simultaneous removal of NO and Hg0 using Fe and Co co-doped Mn-Ce/TiO2 catalysts, Fuel 224 (2018) 241–249.
[120] F. Wang, B. Shen, S. Zhu, Z. Wang, Promotion of Fe and Co doped Mn-Ce/TiO2 catalysts for low temperature NH3-SCR with SO2 tolerance, Fuel 249 (2019) 54–60.
[121] X. Bie, K. Wu, K. Jiao, K. Zhao, X. Chen, S. Ma, Behavior and structure tuning of (Mn&Fe)AlOx-based catalysts for superior denitrification performance, J. Environ. Chem. Eng. 9 (2021), 106153.
[122] L. Li, J. Ji, W. Tan, W. Song, X. Wang, X. Wei, K. Guo, W. Zhang, C. Tang, L. Dong, Enhancing low-temperature NH3-SCR performance of Fe-Mn/CeO2 catalyst by Al2O3 modification, J. Rare Earths 40 (2021) 1454–1461.
[123] N. Zhang, Y. Xin, X. Wang, M. Shao, Q. Li, X. Ma, Y. Qi, L. Zheng, Z. Zhang, Iron-niobium composite oxides for selective catalytic reduction of NO with NH3, Catal. Commun. 97 (2017) 111–115.

[124] W. Zhang, X. Shi, M. Gao, J. Liu, Z. Lv, Y. Wang, Y. Huo, C. Cui, Y. Yu, H. He, Iron-based composite oxide catalysts tuned by CTAB exhibit superior NH3-SCR performance, Catalysts 11 (2021) 224.
[125] W. Zhang, X. Shi, Z. Yan, Y. Shan, Y. Zhu, Y. Yu, H. He, Design of high-performance iron-niobium composite oxide catalysts for NH3-SCR: insights into the interaction between Fe and Nb, ACS Catal. 11 (2021) 9825–9836.
[126] C. Sun, W. Chen, X. Jia, A. Liu, F. Gao, S. Feng, L. Dong, Comprehensive understanding of the superior performance of Sm-modified Fe2O3 catalysts with regard to NO conversion and H2O/SO2 resistance in the NH3-SCR reaction, Chin. J. Catal. 42 (2021) 417–430.
[127] J. Wang, Z. Xu, W. Zhao, X. Li, Selective catalytic reduction of NO by NH3 over MoO3 promoted Fe2O3 catalyst, Kinet. Catal. 59 (2018) 628–634.
[128] G.A.H. Mekhemer, Surface acid–base properties of holmium oxide catalyst: in situ infrared spectroscopy, Appl. Catal. A 275 (2004) 1–7.
[129] K. Zhuang, Y. Zhang, T. Huang, B. Lu, K. Shen, Sulfur-poisoning and thermal reduction regeneration of holmium-modified Fe-Mn/TiO2 catalyst for low-temperature SCR, J. Fuel Chem. Technol. 45 (2017) 1356–1364.
[130] D. Fang, F. He, X. Liu, K. Qi, J. Xie, F. Li, C. Yu, Low temperature NH3-SCR of NO over an unexpected Mn-based catalyst: promotional effect of Mg doping, Appl. Surf. Sci. 427 (2018) 45–55.
[131] L. Xu, S. Niu, C. Lu, Q. Zhang, J. Li, Influence of calcination temperature on Fe0.8Mg0.2Oz catalyst for selective catalytic reduction of NOx with NH3, Fuel 219 (2018) 248–258.
[132] L. Qiu, D. Pang, C. Zhang, J. Meng, R. Zhu, F. Ouyang, *In situ* IR studies of Co and Ce doped Mn/TiO2 catalyst for low-temperature selective catalytic reduction of NO with NH3, Appl. Surf. Sci. 357 (2015) 189–196.
[133] R. Jin, Y. Liu, Z. Wu, H. Wang, T. Gu, Low-temperature selective catalytic reduction of NO with NH3 over MnCe oxides supported on TiO2 and Al2O3: a comparative study, Chemosphere 78 (2010) 1160–1166.
[134] T. Boningari, R. Koirala, P.G. Smirniotis, Low-temperature catalytic reduction of NO by NH3 over vanadia-based nanoparticles prepared by flame-assisted spray pyrolysis: influence of various supports, Appl. Catal. B 140-141 (2013) 289–298.
[135] J. Mosrati, H. Atia, R. Eckelt, H. Lund, G. Agostini, U. Bentrup, N. Rockstroh, S. Keller, U. Armbruster, M. Mhamdi, Nb-modified Ce/Ti oxide catalyst for the selective catalytic reduction of NO with NH3 at low temperature, Catalysts 8 (2018) 175.
[136] L. Chen, J. Yang, S. Ren, Z. Chen, Y. Zhou, W. Liu, Effects of Sm modification on biochar supported Mn oxide catalysts for low-temperature NH3-SCR of NO, J. Energy Inst. 98 (2021) 234–243.
[137] J. Deng, J. Liu, W. Song, Z. Zhao, L. Zhao, H. Zheng, A.C. Lee, Y. Chen, J. Liu, Selective catalytic reduction of NO with NH3 over Mo-Fe/beta catalysts: the effect of Mo loading amounts, RSC Adv. 7 (2017) 7130–7139.
[138] R. Gao, D. Zhang, P. Maitarad, L. Shi, T. Rungrotmongkol, H. Li, J. Zhang, W. J. Cao, Morphology-dependent properties of MnO2 /ZrO2 –CeO2 nanostructures for the selective catalytic reduction of NO with NH3, J. Phys. Chem. C 117 (2013) 10502–10511.
[139] R. Shi, X. Lin, Z. Zheng, R. Feng, Y. Liu, L. Ni, B. Yuan, Selective catalytic reduction of NOx with NH3 over Sb modified CeZrOx catalyst, React. Kinet. Mech. Catal. 124 (2018) 217–227.
[140] H. Chen, Y. Xia, H. Huang, Y. Gan, X. Tao, C. Liang, J. Luo, R. Fang, J. Zhang, W. Zhang, X. Liu, Highly dispersed surface active species of Mn/Ce/TiW catalysts for high performance at low temperature NH3-SCR, Chem. Eng. J. 330 (2017) 1195–1202.
[141] N. Fang, J. Guo, S. Shu, H. Luo, Y. Chu, J. Li, Enhancement of low-temperature activity and sulfur resistance of Fe0.3Mn0.5Zr0.2 catalyst for NO removal by NH3-SCR, Chem. Eng. J. 325 (2017) 114–123.
[142] N. Fang, J. Guo, S. Shu, H. Luo, J. Li, Y. Chu, Effect of calcination temperature on low-temperature NH3-SCR activity and the resistance of SO2 with or without H2O over Fe-Mn-Zr catalyst, J. Taiwan Inst. Chem. Eng. 93 (2018) 277–288.
[143] L.J. France, Q. Yang, W. Li, Z. Chen, J. Guang, D. Guo, L. Wang, X. Li, Ceria modified FeMnOx—enhanced performance and sulphur resistance for low-temperature SCR of NOx, Appl. Catal. B 206 (2017) 203–215.
[144] Y. Zhou, S. Ren, M. Wang, J. Yang, Z. Chen, L. Chen, Mn and Fe oxides co-effect on nanopolyhedron CeO2 catalyst for NH3-SCR of NO, J. Energy Inst. 99 (2021) 97–104.
[145] A. Stahl, Z. Wang, T. Schwaemmle, J. Ke, X. Li, Novel Fe-W-Ce mixed oxide for the selective catalytic reduction of NOx with NH3 at low temperatures, Catalysts 7 (2017) 71.
[146] Z. Xiong, C. Wu, Q. Hu, Y. Wang, J. Jin, C. Lu, D. Guo, Promotional effect of microwave hydrothermal treatment on the low-temperature NH3-SCR activity over iron-based catalyst, Chem. Eng. J. 286 (2016) 459–466.
[147] Y. Hou, J. Wang, Q. Li, Y. Liu, Y. Bai, Z. Zeng, Z. Huang, Environmental-friendly production of FeNbTi catalyst with significant enhancement in SCR activity and SO2 resistance for NOx removal, Fuel 285 (2021), 119133.
[148] F. Li, Y. Zhang, D. Xiao, D. Wang, X. Pan, X. Yang, Hydrothermal method prepared Ce-P-O catalyst for the selective catalytic reduction of NO with NH3 in a broad temperature range, ChemCatChem 2 (2010) 1416–1419.
[149] Z. Si, D. Weng, X. Wu, R. Ran, Z. Ma, NH3-SCR activity, hydrothermal stability, sulfur resistance and regeneration of Ce0.75Zr0.25O2-PO(4)(3-)catalyst, Catal. Commun. 17 (2012) 146–149.
[150] S. Gao, X. Chen, H. Wang, J. Mo, Z. Wu, Y. Liu, X. Weng, Ceria supported on sulfated zirconia as a superacid catalyst for selective catalytic reduction of NO with NH3, J. Colloid Interface Sci. 394 (2013) 515–521.
[151] Z. Ren, H. Fan, R. Wang, A novel ring-like Fe2O3-based catalyst: tungstophosphoric acid modification, NH3-SCR activity and tolerance to H2O and SO2, Catal. Commun. 100 (2017) 71–75.
[152] Z. Ren, Y. Teng, L. Zhao, R. Wang, Keggin-tungstophosphoric acid decorated Fe2O3 nanoring as a new catalyst for selective catalytic reduction of NOx with ammonia, Catal. Today 297 (2017) 36–45.
[153] J. Wu, S. Jin, X. Wei, F. Gu, Q. Han, Y. Lan, C. Qian, J. Li, X. Wang, R. Zhang, W. Qiao, L. Ling, M. Jin, Enhanced sulfur resistance of H3PW12O40-modified Fe2O3 catalyst for NH3-SCR: synergistic effect of surface acidity and oxidation ability, Chem. Eng. J. 412 (2021), 128712.
[154] H. Wang, Y. Ma, X. Chen, S. Xu, J. Chen, Q. Zhang, B. Zhao, P. Ning, Promoting effect of SO2−4 functionalization on the performance of Fe2O3 catalyst in the selective catalytic reduction of NOx with NH3, J. Fuel Chem. Technol. 48 (2020) 584–593.
[155] C. Yang, K. Zhang, Y. Zhang, G.J. Peng, M. Yang, J. Wen, Y. Xie, F. Xia, L. Jia, Q. Zhang, An environmental and highly active Ce/Fe-Zr-SO42- catalyst for selective catalytic reduction of NO with NH3: the improving effects of CeO2 and SO42, J. Environ. Chem. Eng. 9 (2021), 106799.
[156] H. Wang, Z. Qu, L. Liu, S. Dong, Y. Qiao, Promotion of NH3-SCR activity by sulfate-modification over mesoporous Fe doped CeO2 catalyst: structure and mechanism, J. Hazard. Mater. 414 (2021), 125565.
[157] X. Li, K. Li, Y. Peng, X. Li, Y. Zhang, D. Wang, J. Chen, J. Li, Interaction of phosphorus with a FeTiOx catalyst for selective catalytic reduction of NOx with NH3: influence on surface acidity and SCR mechanism, Chem. Eng. J. 347 (2018) 173–183.
[158] K. Zhao, J. Meng, J. Lu, Y. He, H. Huang, Z. Tang, X. Zhen, Sol-gel one-pot synthesis of efficient and environmentally friendly iron-based catalysts for NH3-SCR, Appl. Surf. Sci. 445 (2018) 454–461.
[159] T. Okuhara, N. Mizuno, M. Misono, D.D. Eley, W.O. Haag, B. Gates, Catalytic chemistry of heteropoly compounds. Advances in Catalysis, Academic Press, 1996, pp. 113–252.
[160] C.L. Hill, Introduction: polyoxometalates-multicomponent molecular vehicles to probe fundamental issues and practical problems, Chem. Rev. 98 (1998) 1–2.
[161] S.S.R. Putluru, A.D. Jensen, A. Riisager, R. Fehrmann, Heteropoly acid promoted V2O5/TiO2 catalysts for NO abatement with ammonia in alkali containing flue gases, Catal. Sci. Technol. 1 (2011) 631–637.
[162] N. Mizuno, M. Misono, Heterogeneous catalysis, Chem. Rev. 98 (1998) 199–218.
[163] J. Kaur, I.V. Kozhevnikov, Efficient acylation of toluene and anisole with aliphatic carboxylic acids catalysed by heteropoly salt Cs2.5H0.5PW12O40, Chem. Commun. 21 (2002) 2508–2509.
[164] S.S.R. Putluru, S. Mossin, A. Riisager, R. Fehrmann, Heteropoly acid promoted Cu and Fe catalysts for the selective catalytic reduction of NO with ammonia, Catal. Today 176 (2011) 292–297.
[165] Z. Huang, Y. Hou, Z. Zhu, Z. Liu, Study on the NO reduction by NH3 on a SO42−/AC catalyst at low temperature, Catal. Commun. 50 (2014) 83–86.
[166] X. Yao, Z. Wang, S. Yu, F. Yang, L. Dong, Acid pretreatment effect on the physicochemical property and catalytic performance of CeO2 for NH3-SCR, Appl. Catal. A 542 (2017) 282–288.
[167] Z. Song, Q. Zhang, P. Ning, X. Liu, J. Fan, Z. Huang, Introduction manner of sulfate acid for improving the performance of SO42−/CeO2 on selective catalytic reduction of NO by NH3, J. Rare Earths 34 (2016) 667–674.
[168] J. Beck, R. Müller, J. Brandenstein, B. Matscheko, J. Matschke, S. Unterberger, K. R.G. Hein, The behaviour of phosphorus in flue gases from coal and secondary fuel co-combustion, Fuel 84 (2005) 1911–1919.
[169] C.M.A. Parlett, K. Wilson, A.F. Lee, Hierarchical porous materials: catalytic applications, Chem. Soc. Rev. 42 (2013) 3876–3893.
[170] L. Zhang, L. Shi, L. Huang, J. Zhang, R. Gao, D. Zhang, Rational design of high-performance DeNOx catalysts based on MnxCo3–xO4 nanocages derived from metal–organic frameworks, ACS Catal. 4 (2014) 1753–1763.
[171] X. Wang, W. Wen, J. Mi, X. Li, R. Wang, The ordered mesoporous transition metal oxides for selective catalytic reduction of NOx at low temperature, Appl. Catal. B 176-177 (2015) 454–463.
[172] Y. Cheng, J. Liu, Z. Zhao, W. Song, Y. Wei, A new 3DOM Ce-Fe-Ti material for simultaneously catalytic removal of PM and NOx from diesel engines, J. Hazard. Mater. 342 (2018) 317–325.
[173] Y. Li, W. Liu, R. Yan, J. Liang, T. Dong, Y. Mi, P. Wu, Z. Wang, H. Peng, T. An, Hierarchical three-dimensionally ordered macroporous Fe-V binary metal oxide catalyst for low temperature selective catalytic reduction of NOx from marine diesel engine exhaust, Appl. Catal. B 268 (2020), 118455.
[174] J. Guo, G. Zhang, Z. Tang, J. Zhang, Design of Prussian blue analogue-derived double-cone structure Ce-Fe catalysts and their enhanced performance for the selective catalytic reduction of NOx with NH3, New J. Chem. 44 (2020) 21244–21254.
[175] C.Y. Huang, R.T. Guo, W.G. Pan, X. Sun, S.W. Liu, J. Liu, Z.Y. Wang, X. Shi, SCR of NOx by NH3 over MnFeOx@TiO2 catalyst with a core-shell structure: the improved K resistance, J. Energy Inst. 92 (2019) 1364–1378.
[176] Y. Li, Y. Hou, Y. Zhang, Y. Yang, Z. Huang, Confinement of MnOx@Fe2O3 core-shell catalyst with titania nanotubes: enhanced N2 selectivity and SO2 tolerance in NH3- SCR process, J. Colloid Interface Sci. 608 (2021) 2224–2234.
[177] S. Cai, H. Hu, H. Li, L. Shi, D. Zhang, Design of multi-shell Fe2O3@MnOx@CNTs for the selective catalytic reduction of NO with NH3: improvement of catalytic activity and SO2 tolerance, Nanoscale 8 (2016) 3588–3598.
[178] Z. Gong, S. Niu, Y. Zhang, C. Lu, Facile synthesis of porous α-Fe2O3 nanostructures from MIL-100(Fe) via sacrificial templating method, as efficient catalysts for NH3-SCR reaction, Mater. Res. Bull. 123 (2020), 110693.
[179] X. Zhou, F. Yu, R. Sun, J. Tian, Q. Wang, B. Dai, J. Dan, H. Pfeiffer, Two-dimensional MnFeCo layered double oxide as catalyst for enhanced selective catalytic reduction of NOx with NH3 at low temperature (25-150 °C), Appl. Catal. A Gen. 592 (2020), 117432.

[180] X. Yu, L. Wang, M. Chen, X. Fan, Z. Zhao, K. Cheng, Y. Chen, Z. Sojka, Y. Wei, J. Liu, Enhanced activity and sulfur resistance for soot combustion on three-dimensionally ordered macroporous-mesoporous MnxCe1-xOδ/SiO2 catalysts, Appl. Catal. B 254 (2019) 246–259.
[181] J. Xu, J. Liu, Z. Zhao, C. Xu, J. Zheng, A. Duan, G. Jiang, Easy synthesis of three-dimensionally ordered macroporous La1−xKxCoO3 catalysts and their high activities for the catalytic combustion of soot, J. Catal. 282 (2011) 1–12.
[182] Y. Wei, J. Liu, Z. Zhao, Y. Chen, C. Xu, A. Duan, G. Jiang, H. He, Highly active catalysts of gold nanoparticles supported on three-dimensionally ordered macroporous LaFeO3 for soot oxidation, Angew. Chem. Int. Ed. 50 (2011) 2326–2329.